ABSTRACT

Identification of Dysregulated miRNA Targets in Human Prostate Cancer

Po-hsun (Patrick) Chen, Ph.D.

Mentor: Alex W. Tong, Ph.D.

MicroRNAs (miRNAs) are small, non-coding RNAs (18~24 nt) that regulate diverse cell functions in mammalian cells, including proliferation, differentiation, metabolism, stress resistance, and death. There is increasing evidence that altered expression and function of regulatory miRNAs contribute to the uncontrolled growth of human cancers. We examined the hypothesis that miRNA expression profiles can distinguish malignant from normal tissues. With the use of high throughput, liquid phase hybridization analyses (mirMASA) were carried out with 40 Stage 1c/2 prostate cancer specimens, using 114 miRNA-specific probes. We identified 5 miRNAs (miR -23b, -100, -145, -221, and -222) that were significantly downregulated in malignant prostate tissues as compared with their normal counterpart from the same patient. Decreased expression was confirmed by quantitative real-time PCR (qRT-PCR) analyses. The pathophysiological role of these downregulated miRNAs was further characterized in the prostate cancer LNCaP cell line, which exhibited similarly reduced expression of miR-23b, -145, -221, and -222. Ectopic expression of mature miR-23b and miR-145 reduced

LNCaP cell growth by >40%. In contrast, transfection with a miRNA (miR-141) that was upregulated did not markedly affect cancer cell growth. The altered expression of miR-145 was of particular interest, in view of its similarly reduced expression in breast, cervical, colon, and lung carcinomas. *In silico* search (TargetScan) yielded 396 eligible targets for miR-145, of which 6 were markedly upregulated in LNCaP cells. These include the prostaglandin F receptor (PTGFR), transforming growth factor (TGFBR2), p21-activated kinase 7 (PAK7), SLIT-ROBO Rho GTPase activating protein 2 (SRGAP-2), kinesin family member 3A (KIF3A), and Ras association (RalGDS/AF-6) domain family 2 (RASSF2). miR-145 was uniformly downregulated in all prostate caner lines tested (LNCaP, 22Rv1, PC-3, Du-145, as compared with the nonmalignant prostate line RWPE-1) This miRNA may be differentially expressed in androgen dependent (AD) and androgen independent (AI) prostate cancer cell lines according to qPCR analysis. Mean expression level of miR-145 was approximately 6-fold lower in AD (LNCaP, 22Rv1) than AI (PC3, Du-145) lines. qPCR analysis suggests that PTGFR and RASSF2 were upregulated in 3 of 4 prostate cancer cell lines, whereas MYCN was only upregulated in androgen independent cell lines. The expression of CCND2, MAP3K3 and MAP4K4 were not significantly upregulated by qPCR analysis. These findings suggest that altered miR-145 expression may impact prostate cancer growth through its loss of regulation of PTGFR and/or RASSF2 activities. qPCR analysis of miR-145 treated prostate cancer cells showed decreased expression of PTGFR and RASSF2 indicating these two genes are potential targets of miR-145 modulation. Direct binding only showed moderate reduction of RASSF2 and a more pronounced reduction of PTGFR. These studies suggest that miR-145 may modulate prostate cancer cell growth by modulating PTGFR activity.

Identification of Dysregulated miRNA in Targets in Human Prostate Cancer

by

Po-hsun (Patrick) Chen, B.S., M.S.

A Dissertation

Approved by the Institute of Biomedical Studies

_____
Robert R. Kane, Ph.D., Director

Submitted to the Graduate Faculty of
Baylor University in Partial Fulfillment of the
Requirements for the Degree
of
Doctor of Philosophy

Approved by the Dissertation Committee

_____
Alex W. Tong, Ph.D., Chairperson

_____
John E. Connolly, Ph.D.

_____
Joseph T. Newman, Ph.D.

_____
Christoper M. Kearney, Ph.D.

_____
Myeonwoo Lee, Ph.D.

Accepted by the Graduate School
December 2009

_____
J. Larry Lyon, Ph.D., Dean

Page bearing signatures is kept on file in the Graduate School.

Copyright © 2009 by Po-hsun Chen

All rights reserved

TABLE OF CONTENTS

List of Figures v

List of Tables vi

List of Abbreviations vii

Acknowledgments ix

Dedication x

Chapter

1. Introduction

Prostate Cancer – The Disease 1

The MicroRNA Phenonmenon 4

MicroRNAs and Cancer 7

Hypothesis 11

2. Profiling of MicroRNAs Expression Patterns in Human Prostate Cancer 13

Material and Methods 15

Results 21

Discussion 32

3. Growth Inhibition Properties of MicroRNAs 36

Material and Methods 37

Results 39

Discussion 44

4. Target Predictions and Validation of MicroRNAs 47

Material and Methods 50

Results 55

Discussion 62

5. Conclusions and Future Studies 68

Appendices

Appendix A – Trypan Blue Assay 72

Appendix B – miR-145 Transfection of LNCaP Cells 74

Appendix C – PCR Conditions for psi-PTGFR and psi-RASSF2 Cloning 77

Appendix D – Sequences 80

Appendix E – UT Southwestern Affymetrix Gene Array 83

Appendix F – Transfection Efficiency 87

Appendix G – qPCR Validation of miRNA Expression in Relapse vs Non-relapse patients 88

References 90

LIST OF FIGURES

Figure		
1.1	miRNA Biogenesis	6
2.1	Comparative Analysis of the miRNA Expression in Cryopreserved and FFPE LNCaP Human Prostate Cancer Cell Line	22
2.2	miRNAs with Significantly Differentiated Expression	24
2.3	Scatterplot of Patient T/N Ratios	25
2.4	Endogenous miRNA Expression of 114 miRNAs in Prostate Cancer	30
3.1	miRNA Reconstitution Effect on Prostate Cancer Cell Growth by Trypan Blue	42
3.2	miR-145 Reconstitution Effect on Prostate Cancer Cell Growth by MTT	43
4.1	miR-145 Target Identification Strategy	49
4.2	Heat Map of mRNA Expression in Prostate Cell Lines	55
4.3	Target Gene Expression by qPCR in Prostate Cancer Cells as Compared to Normal Prostate Epithelial Cells, RWPE-1	57
4.4	*PTGFR* and *RASSF2* Expression 24 Hours Post miR-145 Transfection in LNCaP Cells	59
4.5	Luciferase Reporter Experiments in Androgen Dependent Cell Lines LNCaP and 22Rv1	61

LIST OF TABLES

Table		
1.1	miRNA Expression in Different Cancers	9
2.1	Patient Population Statistics	16
2.2	Altered miRNA Expression in Human Prostate Cancer	26
2.3	miRNA Expression as Determined by mirMASA and qRT-PCR	28
2.4	Differential miRNA Expression in Chemical Relapse and Non-Relapse Prostate Cancers	30
3.1	miRNA Expression in the LNCaP Cell Line	40
4.1	Available Programs for miRNA Target Predictions	48
4.2	Increased Expression of miR-145 Target Genes	56

LIST OF ABBREVIATIONS

bp	Base pairs
cDNA	Complementary deoxyribonucleic acid
CRAd	Conditionally replicating adenovirus
DNA	Deoxyribonucleic acid
FBS	Fetal bovine serum
fg	Femtograms
FGC	Fast growing clone
MFI	Mean fluorescent intensity
mg	Milligram
mL	Milliliter
MTT	3-[4,5-dimethlythiazol-2-yl]-2, 5-diphenyltetrazolium bromide
N	Normal
ng	Nanograms
nM	Nanomolar
nt	Nucleotides
PCa	Prostate cancer
PCR	Polymerase chain reactions
PTGFR	prostaglandin F receptor
qPCR	Quantitative PCR
RASSF2	Ras association (RalGDS/AF-6) domain family 2

RLU	Relative luciferase units
SD	Standard deviation
T	Tumor
UNT	Untreated
UTR	Untranslated region
µg	Microgram
µL	Microliter

ACKNOWLEDGMENTS

I thank Baylor University and the department of Biomedical Studies for giving me the opportunity to attend their exceptional graduate program. I especially would like to thank Dr. Darden Powers for his support and encouragement for me to attend the Ph.D. program, Dr. Robert Kane, the current Director of the Institute of Biomedical Studies, for his continued support as well as mediation between the students and administration.

I owe an enormous debt of gratitude to my mentor, Dr. Alex W. Tong, for being patient and encouraging throughout my PhD training. I thank him for opening my eyes to the world of research and challenging me to strengthen or build my ability to develop ideas, design experiments, and complete experiments independently, as well as the ability to be critical in interpreting results. I also appreciate his guidance to overcome obstacles and for his installation on the thought process of problem solving.

I also thank my dissertation committee members, Dr. Alex W Tong, Dr. Joseph Newman, Dr. Myeongwoo Lee, Dr. Chris Kearney, and Dr. John Connolly, for their time, recommendations, and contributions to my dissertation. Dr. Joseph Newman for critiquing and encouragement throughout my years of study, especially for his enthusiastic support at times of need.

I thank Dr. Chris Jay, for his help during the initiation of my dissertation project, as well as him insight for data base generation and result interpretation. Without his support, this dissertation project would not have been completed so successful. I owe

an enormous of gratitude to him for engaging me in critical thinking as well as understanding the results that we generated.

I also thank the personnel at Gradalis Inc, Ila Oxendine, Dr. Vincent Wang, Dr. Donald Rao, Padmasini Kumar, for their help, friendship and moral support. My classmates: Shengnan (Nancy) Liu for her help and Lindsay Butcher, for their constant support and encouragement. My lab mates: Dr. Anagha Phadke, Salina Chen, and Dr. William Xia, for their presence when I needed advice.

I appreciate my good friends Graham Wong and Albert Lai for their companionship and support. Without them, this experience would have not been complete. My long time best friend, John Cheng, for always being there for me when I needed someone to uplift my spirits.

My deepest gratitude goes to my family for their endless support. My parents for being there, both financially and morally, as well as their love even though at times I am not the easiest person to deal with. My dad for being a voice of reason and fundamentals, and most of all for keeping me focused. My mom for listening to my complaints, and providing me with the strengthen to complete my goal. I appreciate my sister for constant reminder that no matter what happens I still have my family. My brother-in-law for his cheerful support. To my best friend and significant other, Shan for her love and patience even at times when I am unbearable, and most important of all for pushing me to continue forward.

DEDICATION

To my parents,

Chi-Min Chen and Shu-Ching Chen (Tung)

CHAPTER ONE

Introduction and Background

Prostate Cancer - The Disease

In 2008, it is estimated that 186,000 new patients will be diagnosed with prostate cancer (PCa), with 28,000 expected deaths (ACS Facts and Figures 2008). Prostate cancer is the most frequently diagnosed cancer in males and the second leading cause of death in the United States with higher incident rates in African-Americans (ACS Facts and Figures 2008). During the early stages of prostate cancer patients are usually asymptomatic, which is the main reason many patients are undiagnosed until the disease reaches a more advanced stage, especially in patients with lower income that cannot afford medical insurance. Symptoms of late stage PCa include weak or interrupted urine flow, bloody urine, frequent urination (unable to control urine flow), and pain during urination (ACS website).

Although researchers have not fully understood the causes of prostate cancer, risk factors have been identified (ACS Complete Guide to PCa, 2005). Age is the strongest risk factor, with rare occurrence in males before the age of forty, but the chances of being diagnosed with prostate cancer quickly increases after fifty. Prostate cancer is more common in North America, Europe, Australia, and the Caribbean islands, but less common in Asia, Africa, Central America, and South America. Lifestyle changes might also have an influence in prostate cancer risks; an example of this is the higher risk of

second generation Asians living in the United States than men living in Asia, who continued to have lower risks of prostate cancer compared to white Americans.

For healthy male adults, only small amounts of PSA (Prostate Specific Antigen) is found in blood, with most men having less than 4 ngs / mL of blood. A patient with a PSA level of 4 -10 ngs / mL have a 25% chance of having prostate cancer, which increases to a 50% chance for patients that have over 10 ngs / mL. There are 2 major forms of PSA in blood, one is attached to blood proteins, while the other circulates freely. This free-PSA can be used to measure percent-free PSA (fPSA), a ratio of how much free-PSA is circulating compared to the total-PSA level. This is useful since men who do not have prostate cancer have lower free-PSA circulating in blood.

Once a patient is diagnosed with prostate cancer, PSA values in conjunction with clinical examinations and biopsies can help the doctor decide whether to do further tests such as CT scans and bone scans are needed. PSA levels can also help determine whether the patient is at risk of the cancer spreading beyond the prostate gland, usually signified by a very high PSA value, this information will alter treatment options. After successful surgery to remove the prostate gland, or radiation therapy, observing PSA levels can help determine if a patient's cancer has relapsed or not since after removing all cancer cells the PSA level drops drastically. These are the main reasons why PSA still remains one of the most important diagnostic, progression, and treatment response markers for prostate cancer. The disadvantages of using PSA values are that its high false negative frequency, giving a normal reading when cancer is present in the prostate, and its false positive rate (25-30%), which falsely diagnosis a normal patient with prostate cancer. When a patient is falsely diagnosed with prostate cancer based on PSA

levels, it can lead to a biopsy even though it is not needed. Therefore; a more accurate and sensitive diagnostic marker is needed.

Standard treatments for prostate cancer include radical prostatectomy, radiation therapy, and hormone therapy. Radical prostatectomy involves the use of a surgical procedure to remove the prostate gland that sometimes damage surrounding nerves. Patients treated with radiation or hormonal therapy also have an increased risk of impotence as well as urinary problems, including leakage and frequent urination. Currently, there is no cure for late stage prostate cancer. The shortcoming of current treatments emphasizes the need for novel biotherapies for the experiment treatment of prostate cancer.

The MicroRNA Phenomenon

MicroRNAs (miRNAs) are small non-coding RNAs (18~24 nt) that were first discovered in *C. elegans* (Lee, Feinbaum et al. 1993). Following the identification of *lin-4, let-7* was identified in a large number of species, including vertebrates. Since then, numerous miRNAs have now been in discovered in higher eukaryotes (Calin, Croce et al. 2006), and exhibit diverse post-transcriptional gene regulatory activities including proliferation, differentiation, metabolism, stress resistence, and death (Lau, Lim et al. 2001; Ambros 2003; Harfe 2005). It is currently estimated that 33% of all gene coding mRNAs are negatively regulated by miRNAs in mammalian cells (Harfe 2005; Calin, Croce et al. 2006; Xi, Shalgi et al. 2006).

miRNA post-transcriptional gene silencing utilizes a mechanism that is similar RNA interference, a function previously thought to be exclusively mediated by small interfering RNAs (Zeng, Yi et al. 2003). The difference between miRNA and siRNA is

that miRNAs are generated from an endogenous transcript whereas siRNAs are generated from exogenous dsRNA molecules. miRNAs also differ from siRNA in its ability to silence gene expression through a cleavage independent manner (Tong, Nemunaitis 2008). Mammalian miRNAs are transcribed in the nucleus by RNA polymerase II (Pol II) as large, polycistronic primary miRNAs (pri-miRNA) precursors that are capped and polyadenylated (Figure 1.1). This pri-miRNA is then processed in the nucleus by Drosha (an RNase III enzyme) and its co-factor, Pasha, into pre-miRNAs, of approximately 70 nucleotides in length and configured in a stem-loop (hairpin) structure. This ~70 nucleotide stem-loop is exported from the nucleus into the cytoplasm by the carrier protein Exportin 5, and also involves Ran, a GTP cofactor (Saestrom, Snove et al. 2006). Exportin 5 binds to its target at high Ran-GTP levels, and releases its payload when GTP is hydrolyzed from Ran (Bohnsack, Czaplinski et al. 2004). Once in the cytoplasm, an RNase III enzyme, Dicer, cleaves the pre-miRNA into a ~22 nucleotide double-stranded miRNA duplex. The miRNA biogenesis is outlined in figure 1.1. This miRNA duplex is inserted in a miRNA associated multiprotein RNA-induced silencing complex (miRISC) similar to that of the RNA induced silencing complex (RISC) as seen in siRNA-mediated mRNA silencing. This complex contains a class of proteins that belong to the Argonaute family. The antisense strand of the duplex guides the RISC complex to bind to the complimentary mRNA target with the appropriate sequence to achieve either transciptional or translation silencing (Khvorova, Reynolds et al. 2003). This multifunctionality is a unique feature of miRNA-mediated, gene silencing (Tong, Nemunaitis et al. 2008), where the downregulation of gene expression occurs through either a cleavage dependent or independent mechanism.

miRNA can induce target mRNA cleavage through a perfect or near perfect sequence complementation with the target mRNA. A perfect complementarity causes the miRISC complex to cleave the mRNA, whereas a imperfect match leads to a protein translational blockade. This protein translational blockade is thought to be the predominant mechanism by which miRNAs function in mammalian cells (Pillai, 2006; Tang 2005). Deadenylation and the subsequent mRNA degradation is another mechanism for the downregulation of mRNA targets from imperfect miRNA binding (Wu, Fan et al. 2006; Giraldez, Mishima et al. 2006).

miRNAs and Cancer

It is predicted that human genome expresses about a thousand different miRNAs, which are thought to regulate at least 30% of genes (Cho 2007). Currently approximately 500 miRNAs have been identified in humans. Only a handful of miRNAs have been associated with their cellular function and role in the development of diseases. Current studies indicate that miRNAs can function as tumor suppressors or oncgenes. Tumor suppressor miRNAs function by negatively regulating genes that promote tumorgenesis. Similarly, miRNAs can also function as oncogenes by downregulating expression of genes that promote tumor suppression.

The ability to silence through imperfect sequence complementation implies that a single miRNA can potentially regulate more than one mRNA target. Using in silico sequence analysis, multiple binding sites in the 3' -UTRs of different mRNAs have been predicted for an individual miRNA. This leads to the multifunctional gene regulation hypothesis that a single miRNA can modulate multiple targets, and multiple miRNAs can modulate a single mRNA. An example of this is the let-7 miRNA where is

dysregulated in many different types of cancers. Johnson and coworkers showed that cell cycle regulators *CDK6* (cyclin D kinase 6) and *CDC25A* are both possible direct targets of let-7 (Johnson, Esquela-Kerscher et al. 2007).

Most tumors expressed lower levels of miRNAs (Lu, Getz et al 2005; Gaur, Jewell et al. 2007). This lowered miRNA expression mimics that of early mammalian development, where the cells are continually dividing and the expression of miRNAs are lower. In cases where overexpressed miRNAs downregulate the transcripts of tumor suppressor genes, these miRNAs are considered as oncogenic miRNAs. Conversely, tumor suppressor miRNAs such as let-7 downregulate the expression of oncogenes, namely *Ras*. Akao and colleagues first showed that the reintroduction of *let-7a-1* into a *let-7* low-expressing colon cancer cell line resulted in significant growth reduction (Akao, Nakagawa et al. 2006). It is now known that miRNAs are often encoded in regions prone to cancer-associated alterations (Calin, Sevignan et al. 2004). Many epithelial cancers have altered microRNA expressions when compared with normal tissue (Lu, Getz et al. 2005; Volinia, Calin et al. 2006) as summarized in Table 1.1 that showed examples of the current known miRNAs and their relationship with different cancers. The ability for miRNAs to function both as a tumor suppressor gene or oncogene and its expression in fragile sites and genomic regions that are often mutated in cancers are important considerations for investigating the miRNA's expression in cancers.

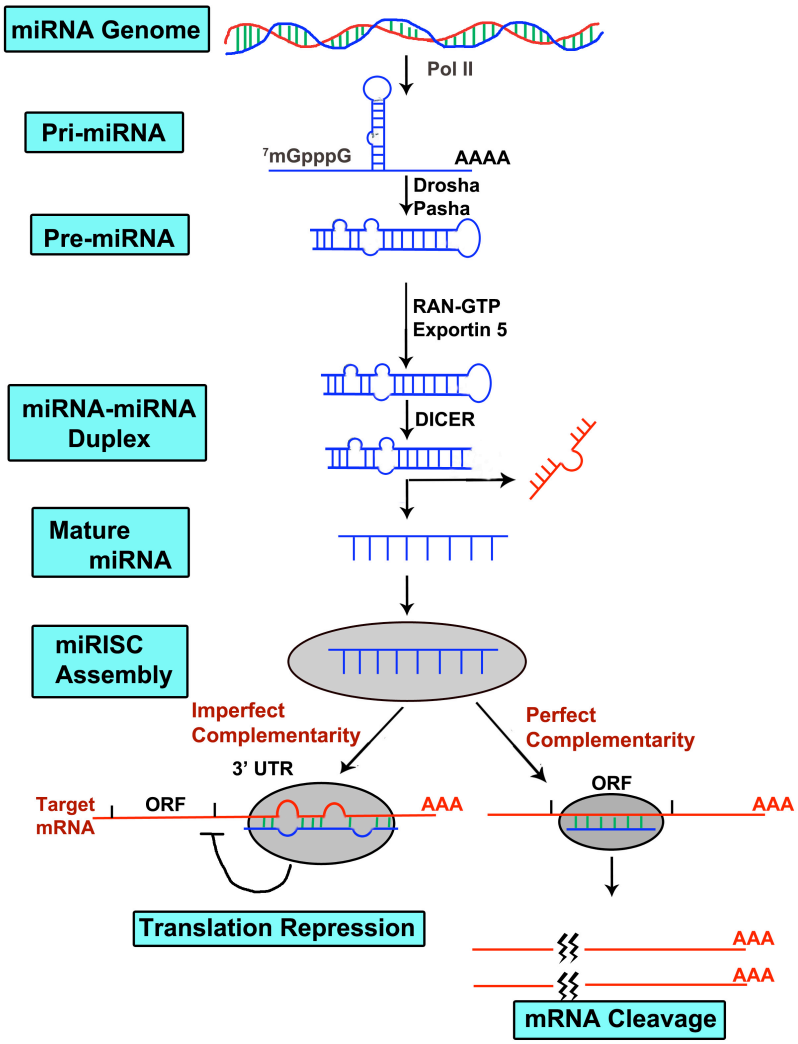

Figure 1.1: miRNA BiogenesismiRNAs are expressed endogenously. A RNA polymerase II transcripts endogenous miRNA into a polycistronic primary miRNA (pri-miRNA), which is then processed by Drosha and its cofactor Pasha in the nucleus into multiple precusor miRNAs (pre-miRNA) that are about ~70 nt in size. These hairpin structured pre-miRNA are exported into the cytoplasm by RAN-GTP dependent Exportin 5. In the cytoplasm, the RNase III enzyme Dicer cleaves the pre-miRNA into duplex miRNAs (22 bp). The duplex miRNA is unwound, and the effector strand is incorporated into the RNA induced silencing complex (RISC) and guides the complex to target mRNAs. Silencing occurs in either a cleavage dependent mechanism, when there is perfect complementarity, or a cleavage independent mechanism, where there is imperferct complementarity.

The roles of miRNAs in cancers and its involvement in the normal stable-status maintenance of cellular functions have many potential applications in disease diagnosis, prognosis, and clinical therapeutic. Although current research has shown the potential application of miRNA expression profiling in complementing diagnostics, a better understanding of the miRNA gene control networks are needed for their clinical applications.

The sudden interest in miRNA profiling in cancers has increased exponentially, a simple PubMed search with "miRNA profiling" reveals that in 2007 there were 218 publications compared to 458 publications in 2008 on miRNA profiling. With this newly developed interest in miRNA profiling in cancers, there is a need to take the technical limitations of current methods in profiling miRNAs into consideration.

In Nelson's recent review published in 2008, he reviews the technical variables in high-throughput miRNA expression profiling that need to be addressed before miRNA gene expression profiling platforms (miGEP) results can considered valid and reliable (Nelson, Wang et al. 2008). He suggests that we use the lessons learnt from mRNA gene expression profiling as a blueprint to optimize current miGEPs. In the early stages of mRNA gene expression profiling many issues on have risen including data reliable as different microarray profiling techniques provided different results, and these differences are even greater between separate laboratories (Wang, He et al. 2005). In a similar way, miRNA expression profiling expresses variable results from different techniques (Nelson, Wang et al. 2008). In Nelson's review, he mentions several technical parameters that need to be addressed these include tissue processing, RNA isolation, result validation using an alternate method and data normalization before we

Table 1.1: miRNA Expression in Different Cancers

Cancer	Increased miRNA	Decreased miRNA	Reference
Chronic lymphocytic lymphoma	miR-15a- miR-16-1 miR-143 miR-145	miR-23b miR-24-1 miR-146 miR-155 miR-195 miR-221	Calin et al. 2002, 2004, 2005 Esquela-Kerscher and Slack, 2006
Breast	miR-21 miR-155	miR-125b miR-145	Iorio et al. 2005
Colorectal	miR-19a miR-21	miR-31 miR-96 miR-133b miR-143 miR-145	Akao et al. 2006 Bandres et al. 2006 Michael et al. 2003 Volinia et al. 2006
Glioblastomas	miR-21 miR-221	miR-181a miR-181b miR-181c	Ciafre et al. 2005 Chan et al. 2005
Hepatocellular carcinoma	miR-18 miR-224	miR-125a miR-195 miR-199* miR-199a miR-200a	Murakami et al. 2006
Prostate	miR-21 miR-141	let-7 family miR-15a miR-16-1 miR-23b miR-26 miR-29 miR-30 miR-99 miR-125b miR-143 miR-145 miR-200 miR-221 miR-222	Esquela-Kerscher and Slack 2006 Ozen et al. 2007 Tong et al. 2008 Volinia et al. 2006
Thyroid	miR-146 miR-221 miR-222		He et al. 2005

can overcome some of the technical difficulties or biases that are currently observed in miRNA expression profiling publications (Nelson, Wang et al. 2008). Taking these technical variables into considerations, current miRNA expression profile appears to still be in its early developmental stages and needs more quality control and consistency before these results can be used for diagnosis and prognosis of cancers. Therefore, the focus of this dissertation is not to predict prostate cancer or whether a patient is likely to relapse using a high-throughput method but to investigate the functions of dysregulated miRNAs and its targets in prostate cancer.

Hypothesis

Altered miRNA expression in prostate cancer tissues impacts oncogenesis and disease progression.

Study Rationale and Specific Aims

1. To identify the dysregulated miRNA profile in prostate cancer.

   We will examine the expression of 114 miRNAs in 40 formalin-fixed paraffin embedded (FFPE) prostatectomy specimens using a high-throughput hybridization assay, in order to identify miRNAs that are dysregulated in prostate malignant tissue. Of these 40 specimens, 20 were of early chemical relapse and 20 non-relapse patients. Our findings will be confirmed by quantitative real-time PCR (qPCR) analysis.

2. To determine growth physiologic outcome of downregulated miRNAs.

   Transient expression of significantly downregulated miRNAs can impact the growth of prostate cancer cells showing its involvement in cancer oncogenesis. In this study, we examine LNCaP cells treated with dysregulated miRNAs to

determine whether the downregulated expression of miRNAs in malignant prostate cancer tissues may impact the pathophysiology of prostate cancer by altering cell growth.

3. To identify molecular target of a miRNA that impacts prostate cancer growth.

   By expressing the miRNA target-sequence in a reporter gene assay, we can investigate the direct binding miRNA and its target. In this study, we examine the endogenous expression of miR-145 predicted target genes by microarray analysis. Our findings will be confirmed by the qPCR assay to show silencing of the PTGFR and RASSF2 mRNA by miR-145. Further, we investigate the interaction of miR-145 with its target genes, PTGFR and RASSF2 using a gene reporter assay.

CHAPTER TWO

Profiling of MicroRNA Expression Patterns in Human Prostate Cancers

Prostate cancer is the most common cancer in man and the second leading cause of death in the United States (ACS Facts and Figures 2008). It is estimated that 186,000 new cases will be diagnosed in 2008, with 28,000 expected deaths. Patients who present with localized disease may be cured through radical prostatectomy or irradiation, albeit with considerable negative impact on health-related quality of life. A subset of these patients, however, is prone to disease relapse, and yet histologically indistinguishable from others with a more benign clinical course. Both preoperative prostate-specific antigen (PSA) velocity and PSA doubling time have been used as predictors of biochemical progression, clinical progression, and death from prostate cancer (Walczak, Carducci et al. 2007). However, a significant number of potentially aggressive prostate cancers may go undetected in men with low/normal PSA values, indicating the need to develop biomarkers that can potentially supplement or even replace PSA for the diagnosis and prognosis of prostate cancer (Bradford, Tomlins et al. 2006).

We and others have observed that altered miRNA expression is a common feature seen in human cancers. Most of these altered miRNA are encoded in regions of high chromosomal instability in hematopoietic malignancies and solid cancers (Calin, Sevignani et al. 2004; Gong, Liu et al. 2005; Johnson, Grosshans et al. 2005; Cimmino, Calin et al. 2005).

The ability of miRNAs to funcation as post-transcriptional regulators of cell growth and differential, in conjunction with their markedly lower complexity (an expression database of over 600 miRNAs has been discovered with at least 1000 miRNAs estimated as compared to over 30,000 readouts for coding mRNAs), the elucidation of dysregulated miRNA expressions present an attractive method toward the development of cancer prognosticators and/or experimental treatments.

Recent studies by Lu, Volinia, and coworkers showed that various human epithelial cancers, including prostate cancer, displayed miRNA signatures that differed from their normal counterparts (Tong, Nemunaitis 2008; Lu, Getz et al. 2005; Volinia, Calin et al. 2006). The miRNA expression profile of human breast cancer and hepatocellular carcinoma has been correlated with prognostic, biopathologic features, although it is uncertain whether clinically distinct cancer subsets can be defined by these unique miRNA phenotypes (Iorio, Ferracin et al. 2005; Murakami, Yasuda et al. 2006). We conducted paired miRNA profiling analysis of normal and malignant tissues of prostatectomy specimens from 40 patients diagnosed with stage T2 prostate cancer, in order to characterize the miRNA expression profile in early disease. Differential miRNA expression was explored in patients with early chemical relapse (< 2 yrs post-prostatectomy) and those without clinical relapse for a period more than 10 years. Our findings suggest that altered miRNA expression likely accompanied the prostate oncogenic process, with the early relapse subset earmarked by additional aberrant miRNA features prior to clinical relapse. In our studies, we elected to analyze micro-dissected malignant and normal tissues concurrently from the same patient, with the aim to determine a more precise

miRNA expression pattern in the patient's malignant tissue as compared with his/her normal tissue. As mentioned in Chapter 1, current technical variables act as limitations of using high-throughput miRNA expression profiling to diagnose and predict prostate cancer. The focus of this dissertation and this chapter is to find dysregulated miRNAs that may impact prostate cancer growth through their interaction with specific gene targets.

Material and Methods

Patient Population and Samples

Forty formalin-fixed, paraffin-embedded (FFPE) prostatectomy specimens, with well-documented clinical follow-ups, were provided by Dr. Pat Fulgham (Presbyterian Hospital of Dallas, Dallas, TX), the patient demographics are shown in Table 2.1. Twenty of these prostatectomy specimens were from patients with early chemical relapse (< 2 years post-prostatectomy), and the other twenty were samples from patients without chemical relapse within a period of 10 years. Chemical relapse is defined as having two consecutive elevated PSA values during following visits. The chemical relapse and non-relapse subsets were matched for age at diagnosis (61.8 + 6.1 for non-relapsed vs 59.4 + 8.7 for early-relapse subset) and Gleason score (5.7 + 1.0 vs. 6.2 + 0.6, respectively). PSA level for the relapsed group (11.2 + 7.9) was significantly higher ($p<0.008$) than that of non-relapsed patients (6.0 + 2.7) at time of diagnosis. These demographics are summarized in Table 2.1. All of the 40 patients were clinically staged as T2a or T2b according to the AJCC staging manual, where T2a means a palpable tumor involving 50% or less of 1 lobe, and T2b involves

palpable disease in more than 50% of 1 lobe. For each specimen, areas with more than 80% of the area containing tumor cells, was microdissected from normal areas based on histopathological features. Research protocols involving human subjects were approved by the Institutional Review Board at Baylor University Medical Center and the Presbyterian Hospital of Dallas.

Table 2.1: Patient Population Statistics

Patient Subset[a]	No. of Patients	Age at Dx[b]	PSA at Dx[b]	Gleason Score[b]
Non-relapsed	20	61.8 ± 6.1	6.0 ± 2.7	5.7 ± 1.0
Chemical Relapsed	20	59.4 ± 8.7	11.2 ± 7.9	6.2 ± 0.6

[a]Chemical relapse is defined as having 2 consecutive elevation of PSA levels at the time of follow-up visit. Non-relapsed patients represent the subset of patients without chemical relapse within a period of 10 years post-prostatectomy.

[b]Mean ± SD

RNA Extraction

Total RNA was extracted in parallel from each maglinant and it's paired non-malignant specimen by using a previously established protocol shown to preserve the integrity of small RNAs (FFPE PureLink RNA Isolation Kit, Invitrogen, Carlsbad CA; Jay 2007). Forty 10 micron sections (400 micron in total) of FFPE tissue was harvested for RNA extraction, with an average yield of 10 - 20 µg of total RNA per microdissected specimen. All isolated RNA was quantified based on spectrophotometry 260/280 ratios (NanoDrop ND-1000, Wilmington, DE). RNA integrity was confirmed by electrophoresis using the BioRad Experion RNA StdSens Chip (BioRad, Hercules, CA).

MirMASA Analysis

Multiplex analysis of microRNA expression was carried out using the mirMASA technique (Genaco, Huntsville, AL), based on liquid phase, hybridization reactions with oligonucleotide-probes sets that are conjugated to fluorescent beads. Each color-coded bead or microsphere is covalently linked to capture oligonucleotide sequence and a biotin-labeled (detection) oligonucleotide, which is detected by flow cytometer. The capture oligonucleotide consists of a 12 nt sequence that binds to the 3' end of the miRNA, whilst the remaining 8-10 nt is hybridized to the biotin-labeled oligonucleotide. Quantification of bound miRNA was done by Fluorokine® MultiAnalyte Profiling (xMAP) flow cytometry, using the Luminex technology (Yang, Tran et al. 2001). To increase the specificity and sensitivity of the assay, both capture oligonucleotide and detection oligonucleotide contain lock nucleic acid (LNA) nucleotides (Petersen, Wengel et al. 2003), distinguishes miRNA with even a single nucleotide difference in primary sequence.

Using the above described system, we investigated the expression of 114 miRNAs in the 40 malignant, and paired normal (total of 80 samples). miRNA sequences were obtained from Sanger miRNA registry (http://microrna.sanger.ac.uk/sequences/). The lack of cross-reactivity of each miRNA probe sequences was previously validated with other miRNAs (Barad, Meiri et al. 2004). The hybridization reactions were divided into pre-optimized panels of 10-12 miRNA probes/panel as to further limit the cross-reactivity by separating miRNAs with similar sequences. Each panel was then incubated at 45˚C for 1 hour protected from light with 1 μg of total isolated RNA described above, followed by

incubation with Streptavidin-PE at 45˚C for 10 mins with washing in between. Each panel miRNA set also included a probe for 5S RNA, serving as an internal loading control to normalize the level of miRNA expression during comparison across different panels. To ensure that the probes only dectected mature miRNA sequences, validation studies were performed using equimolar concentrations of precursor and mature miRNAs, miR-15b and miR-17-5p (Yang, Tran et al. 2001). This study showed that the mirMASA probes binds preferentially to mature sequences, whereas the detection of precursor miRNAs was negligible.

Each patient's maglinant and non-maglinant tissue pair was analyzed in parrallel. Quantification of miRNA was expressed as mean fluorescence intensity (MFI) based on minimum of 100 events counted per probe set. For each miRNA, at least 100 probes were counted per sample. The miRNA MFI was then normalized against 5S RNA probe sets to account for sample variations. 5S RNA expression in maglinant tissue (MFI of 8526 ± 678; mean ± stdev, where n = 40) did not differ significantly from their paired non-maglinant tissues (8400 ± 763, n = 40, p = 0.53, Student's two sided t-test). Further statistical analysis showed that the 5S RNA expression also did not differ significantly across different patient maglinant and non-maglinant sample pairs (p = 0.38, n = 40, Student's two sided test). MFI values of samples that were ≥ 2 fold below negative bead-control were set as 0 signifying no expression. Using synthetic miRNAs, the dynamic range of the mirMASA technique was found to be > 2 logs, with a CV of 1.7% and minimum sensitivity of 0.1 fetamols.

Populational Analysis to Differentiate miRNA Expression Comparing Tumor and Normal Tissue

Negative bead-control were first subtracted (background subtraction) from MFI values before normalization against 5S RNA. To then account for zeros and negative numbers in the data set, the population MFI values were normalized by log-transformation using the formula [$x' = \log_2(x+1)$], where x' represents the adjusted value, and x, the observed MFI after background subtraction and 5S normalization. The final values were expressed as the differential miRNA expression as tumor over normal (T/N) ratios. This was achieved by comparing the quantitated normalized MFI value of the miRNA-probe binding activity by tumor (T, maglinant) versus normal (N, non-maglinant) tissue-extracted RNAs for the same patient. The normalized T/N ratios were then exported to the GeneSpring 7.3.1 software (Agilent Technologies, Forest City, CA) for gene hierarchical analysis, which clusters genes with similar expression together. To differentiate miRNAs that had significantly altered expression, between tumor and normal tissue samples, SAM (Significance Analysis of Microarrays) was performed on all 114 miRNAs of the 40 patient tumor, normal pairs. Analysis was performed in Excel using the R statistical package with default SAM parameters. The differential expression of T/N ratios were expressed in heatmaps as a comparison between the expression of miRNAs (Y-axis) versus patients (X-axis). Patient were sorted according to Euclidian distance metric, and the miRNA expression were clustered using hierarchical clustering using standard correlation.

Reverse Transcription and Real Time, qPCR

To quantify patient miRNA, synthetic miRNAs were used as standards. These synthetic miRNAs were commercially synthesized (IDT DNA Synthesis Labs, Coralville, IA) according to the published sequence on the Sangar miRNA database (http://microrna.sanger.ac.uk/sequences/). One hundred nanograms of each tumor/normal paired patient total RNA was extracted from FFPE preserved specimens as previously described. Quantitative real time PCR (qRT-PCR) was divided into two major steps, 1) RNA reverse transcription, and 2) real time PCR using specific TaqMan Probes. The reverse transcription step (TaqMan MicroRNA Reverse Transcription Kit, Applied Biosystems, Foster City, CA) was normalized to 100 ng of starting patient total RNA using pre-qualified miRNA-specific primers (TaqMan MicroRNA Assays, Applied Biosystems, Foster City, CA). The quantitative real time PCR was done using a PCR master mix containing AmpliTaq Gold DNA polymerase (TaqMan Universal PCR Master Mix without AmpErase, Applied Biosystems, Foster City, CA) and miRNA-specific amplification primers (TaqMan MicroRNA Assays, Applied Biosystems, Foster City, CA). The following miRNA expressions were confirmed by qRT-PCR: hsa-miR-20a, -23b, -100, -141, -143, -145, -221, and -222 according to the manufacturer's protocol (95˚C for 10 mins, 40 cycles: 95˚C for 15 sec, 60˚C for 60 sec, Applied Biosystem). Synthetic miRNA standards were defined with a range of 1 ng to 1 fg and were analyzed simultaneously with patient samples to quantify unknown miRNA levels.

Differential Expression Analysis of Chemical-Relapse and Non-Relapse Subsets

The mirMASA T/N findings for each miRNA from previously described methods, was also used to separate relapse and non-relapse patient subsets according to hierarchical analysis. qRT-PCR, as described above, was also carried out to confirm the mirMASA findings using a pool of 13 miRNAs (hsa-miR-16, -23a, -34c, -96, -122a, -129, -135b, -140, -154, -194, -218, -298, -342; TaqMan MicroRNA Assay, Applied Biosystems, Foster City, CA) using commercially available probes. If the miRNA expression was below the simultaneously generated standard curve in four or more patients, the miRNAs were not included in the analysis. These include miRNAs: miR-23a, -34c, -96, -122a, -129, -154, and -298. The relative expressions of each miRNA was expressed as T/N ratios (mean $T/N_{relapse}$ / mean $T/N_{non\text{-}relapse}$).

Results

Human Prostate Cancer Signature by Array Analysis

One of the major obstacles of using formalin-fixed, parafin-embedded (FFPE) preserved specimens is tendency of RNAs to be degraded. Validation studies performed by us and others demonstrated that small RNAs were preserved after the formalin-fixation and paraffin-embedding (FFPE) process (Jay C, DNA Cell Biol 2007; Nelson PT, Nat Methods 2004). In our studies, the miRNA levels were proportionately decreased in FFPE cells, and correlated strongly to miRNA expression levels of the corresponding cryopreserved specimens ($r^2 = 0.93$, $p = 0.0001$). Figure 2.1 shows the miRNA expression trend of cryopreserved and FFPE

LNCaP cells. These findings support the feasibility of utilizing FFPE patient specimens for the quantitive analysis of miRNA expression.

Our current analyses employed archived, FFPE specimens derived from surgically resected prostatectomy procedures performed in the course of treatment for prostate cancer. Individual patient specimens were microdissected into histopathologically-defined malignant and non-malignant subsets. This approach allowed for an internally-controlled comparison of the miRNA expression profile of malignant and non-malignant tissues from each patient. Total RNA harvested from each subset was analyzed in parallel by the mirMASA assay, a liquid phase, multiplex analytical approach utilizing hybridization probes for 114 miRNAs (Lu, Getz et al. 2005; Yang, Tran et al. 2001; Barad, Meiri et al. 2004). Pre-validation studies using synthetic miRNAs showed that SDs for replica determinations were 2-9% of the mean value. Readouts were normalized to the hybridization reaction of 5S RNA, whose expression in tumor and normal tissues of individual patients did not differ significantly from one another ($p=0.38$; Student's two sided paired t test) in our study population. Paired, differential analysis was carried out to arrive at a tumor/normal (T/N) expression ratio for individual miRNAs. The mean populational T/N expression ratio is analyzed statistically against the null hypothesis of a T/N ratio of 1.

More than ninety percent of the 114 probed miRNAs (except miR-207, -211, and -322) displayed a positive hybridization signal in our 40 paired prostate tissues examined. The unamplified levels of the majority of miRNAs were relatively unchanged in malignant tissues as compared to their normal counterpart. However,

nine miRNAs (miR -23b, -24, -100, -125b, -143, -145, -205, -221, and -222) were significantly reduced in malignant prostate cancers, according to hierarchical cluster analysis and the SAM (significance analysis of microarrays) algorithm used to reveal differentially expressed miRNAs (Figure 2.2).

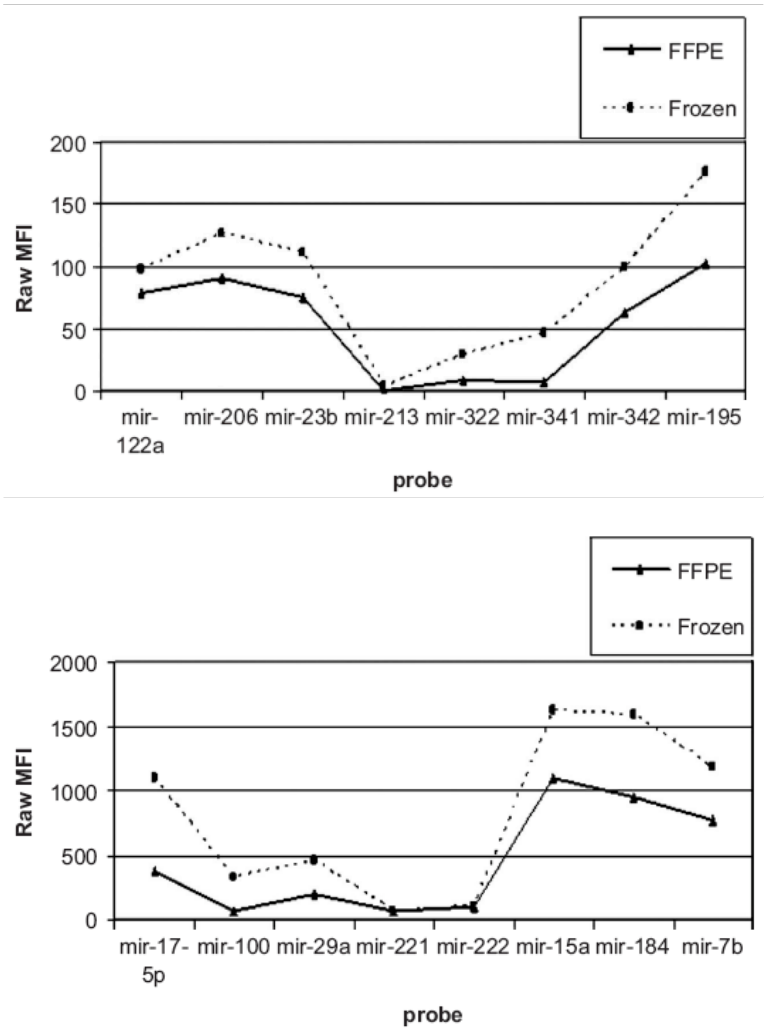

Figure 2.1: Comparative Analysis of the miRNA Expression in Cryopreserved and FFPE LNCaP Human Prostate Cancer Cell Line. Total RNA harvested from cryopreserved or FFPE LNCaP cells was analyzed in parallel with 114 miRNA (only a representation is shown in this figure) by a liquid-phase hybridization technique (mirMASA). miRNA expression profiles from the two RNA sources appeared to be similar, albeit with proportionately lower levels of expression in the FFPE sample

In particular, the decreased expression of a subset of 5 miRNAs (miR -23b, -100, -145, -221, and -222) was validated by the more stringent, paired t-test with Bonferroni correction ($p<0.05$). The T/N values for these reduced miRs in individual 40 patients (each represented as a column) for each miRNA tested (represented in rows) are shown in Figure 2.3. Mean reduced expression ranged from approximately 56% (miR-222) to 24% (miR-100; Table 2.1) in malignant tissues.

Validation of miRNA Expression by Quantitative RT-PCR

To validate the down down-regulation of miR -23b, -100, -145, -221 and -222 in malignant prostate cancer cells, real time quantitative PCR analysis was carried out with miRNA specific primer/probe sets under preoptimized conditions. Primer/probe sets were preselected to exclude precursor miRNA amplification. Twelve patient specimens, six from each clinical subset, were selected for their representative miRNA expression profile as displaying decreased levels of miRs -23b, -100, -145, -221, and -222 by mirMASA. The overall T/N ratios as determined by RT-PCR strongly correlated with mirMASA findings when all 6 miRNAs were analyzed collectively ($p = 0.002$, binomial test).Significant correlations were also demonstrated for individual miRNAs miR -23b, -143, -145, -221, and -222, based on the small numbers of samples tested (mean T/N ratio of 0.84, 0.76, 0.56, 0.85 and 0.62, respectively; Table 2.3), with miR-100 (T/N ratio of 0.89) approaching statistical significance ($p < 0.06$). qRT-PCR analysis confirmed down-regulated miR-100 expression in 4 of 8 patients who exhibited a reduced expression by $\geq$ 20% by mirMASA (Table 2.3). This discrepancy may be partly attributed to the higher sensitivity of the mirMASA assay in discriminating moderate reductions of miRNA

expression (Barad, Meiri et al. 2004). Real time, qRT-PCR also confirmed the up-regulated expression of miR -20a and -141 in 7 of 12, and 10 of 12 malignant prostate tissues tested, and corresponded to an mean increased T/N ratio of 6.69 and 2.58, respectively. As an internal reference correlative control, the expression analysis of let-7f miRNA showed no change between tumor and normal tissue by mirMASA (T/N ratio of 1.0 ± 0.18) or by qRT-PCR (1.1 ± 0.30).

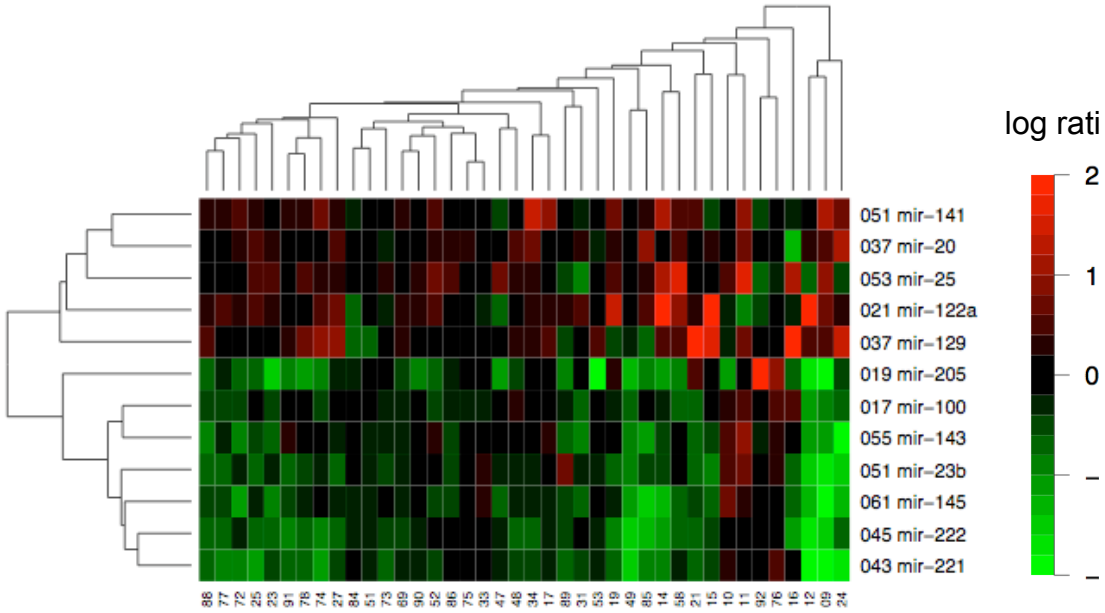

Figure 2.2: miRNAs with Significantly Differentiated Expression. One hundred and fourteen miRNAs were probed against 40 patient malignant and non-malignant samples. A heat map was generated using the expression ratios of 16 miRNAs that differed significantly in malignant vs. non-malignant tissues, according to SAM. Red: up-regulated miRNAs, green: down-regulated miRNAs as compared with non-malignant counterparts. Relatedness in miRNA expression across samples is shown by hierarchical tree on the Y axis via standard linkage. Patient (X-axis) were sorted using Euclidean distance metric.

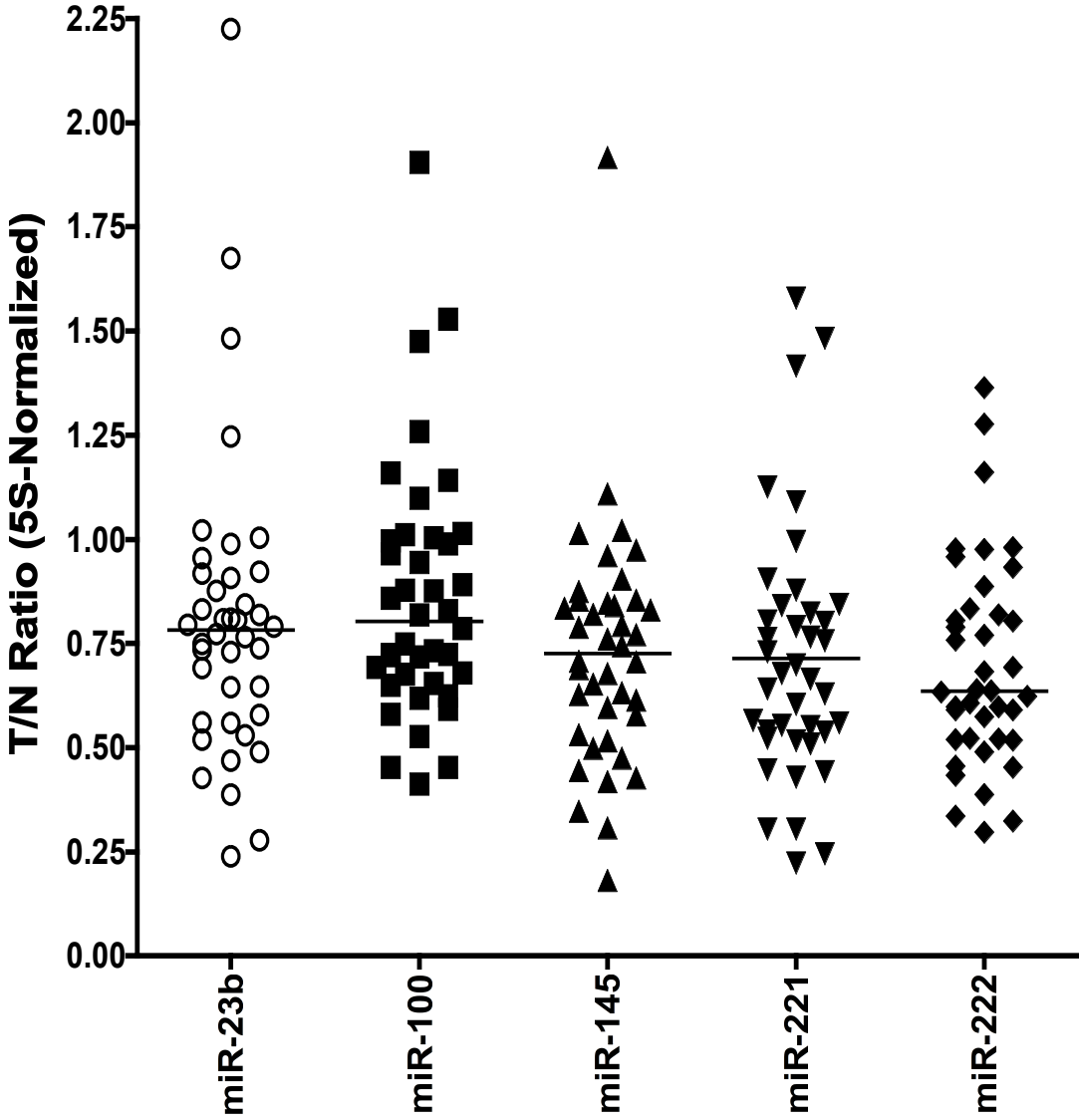

Figure 2.3: Scatterplot of Patient T/N Ratios. Scatterplot of T/N expression ratios for individual patients is shown for miR -23b, -100, -145, -221, and -222, whose expression was found to be significantly decreased, based on population analysis by SAM and paired t test with Bonferroni correction. Expression readouts were normalized to the hybridization reaction of 5S RNA, then subjected to paired, differential analysis to arrive at a tumor/normal (T/N) expression ratio for individual miRNAs. Line represents median expression level for each miRNA.

Table 2.2: Altered miRNA Expression in Human Prostate Cancer

miRNA tested	Relative expression	Statistical Assessments	
	Mean T/N ratio (log_2 T/N ratio)[a]	q value (SAM)	p-value (paired t-test)
Down-regulated miRNAs			
miR-222†	0.68 (-0.56)[b]	0.00	3.95E-09
miR-221†	0.68 (-0.56)	0.00	8.24E-08
miR-145†	0.70 (-0.51)	0.00	5.04E-07
miR-23b†	0.77 (-0.38)	0.00	3.25E-05
miR-100†	0.85 (-0.24)	0.00	2.16E-04
miR-143	0.80 (-0.31)	0.00	6.53E-04
miR-205	0.70 (-0.52)	0.00	1.25E-03
miR-24	0.92 (-0.13)	13.16	1.43E-03
miR-125b	0.88 (-0.19)	10.53	4.93E-03
Up-regulated miRNAs			
miR-141	1.18 (0.24)	6.48	1.06E-03
miR-20a	1.14 (0.19)	6.48	3.54E-03
let-7a	1.14 (0.19)	13.16	7.31E-03
miR-25	1.17 (0.23)	6.48	9.16E-03
miR-129	1.26 (0.33)	6.48	9.78E-03
miR-122a	1.23 (0.29)	6.48	1.36E-02
miR-302	1.16 (0.21)	13.16	1.76E-02

[a]Tumor: normal (T/N) expression ratios represent mean of 40 samples. Values were normalized to 5S expression; values < 1.0 denote decreased miRNA expression in malignant tissues, values > 1.0 represent upregulated miRNA expression.
[b]log_2 T/N ratios shown in parenthesis.
†denotes T/N ratios that are significantly different from 1.0 by paired t test with Bonferroni correction and SAM.

Table 2.3: miRNA Expression as Determined by mirMASA and qRT-PCR

miRNA tested	Mean T/N ratio[a]		
	mirMASA	qRT-PCR	p-value[b]
Down-regulated subset			
miR-23b†	0.803 (-0.317)[c]	0.843 (-0.247)	0.008
miR-100†	0.799 (-0.324)	0.890 (-0.014)	0.063
miR-143	0.878 (-0.187)	0.756 (-0.404)	0.004
miR-145†	0.744 (-0.427)	0.559 (-0.840)	0.0002
miR-221†	0.682 (-0.552)	0.853 (-0.230)	0.001
miR-222†	0.713 (-0.488)	0.618 (-0.694)	0.004
Up-regulated subset			
miR-20a	1.274 (0.349)	6.697 (2.744)	0.008
miR-141	1.379 (0.464)	2.581 (1.368)	0.002
Reference miRNA			
let-7f	1.000	1.100	0.499

[a] Mean tumor: normal (T/N) expression ratios for 6 chemical-relapse and 6 non-relapse patients with a representative miR signature of significantly downregulated miR-23b, -100, -145, -221, -222, according to paired t test with Bonferroni correction and SAM in population analysis (†). miR-143 was included in analysis in view of the expected, linked expression with miR-145.
[b]Concordance of T/N ratios by mirMASA vs. qRT-PCR findings was determined by the formula p=1/2^n, where n is the number of samples that demonstrate a similar direction of change (up or down regulation) by both assays. The combined p value for all miRs = 0.002
[c]$\log_2$ T/N ratios shown in parenthesis.

miRNA Expression Profile in Early Relapse Prostate Cancer

To consider whether clinically aggressive prostate cancers display a distinguishable, predictive miRNA phenotype, differential analysis was carried out to examine the miRNA expression profiles of early chemical-relapse patients with a sequential rise in PSA within 2 yrs of prostatectomy (n=20), as compared with those

without disease relapse for ≥ 10 years (n=20). Following the exclusion of miRNAs that display a similar expression trend across both clinical subsets, the expression profile of 48 miRNAs was used to segregate of 90% of patients with chemical-relapsed disease, according to hierarchical clustering analysis (Figure 2.4). This node excluded 80% of the non-relapse patients, based on heat map distance analysis**.**

Starting with the expression levels of 48 miRNAs (Figure 2.4), support vector machine (SVM) algorithm analyses were carried out to optimize clinical subset separation with a reduced number of miRNAs. A subset of 16 miRNAs produced a similar predictive outcome, segregating 15 of 20 (75%) chemical relapse patients, while excluding 85% (17 of 20) of non-relapse patients (Table 2.4).

miRNA expression was confirmed using qPCR (with a pool of 13 miRNAs including: hsa-miR-16, -23a, -34c, -96, -122a, -129, -135b, -140, -154, -194, -218, -298, -342) on the same, patient biopsies that yielded adequate amounts of RNA (n = 11 for each clinical subset). We identified a concordance of upregulated expression of miR-16, miR-135b, miR-194, and miR-218, and downregulated miR-140. Regardless of whether the T/N ratio was determined by mirMASA or qPCR, miRNA expression did not significantly differ in either method ($P > 0.05$, Student's two-tailed paired t-test). Our results by qPCR showed that miR-135b (R/NR ratio of 1.6) and miR-194 (1.4) had more than 40% differential expression between the relapse (R) and non-relapse (NR) patient subsets even though the difference was not statistically significant ($p > 0.05$, Mann-Whitney test, Appendix G). The limited patient samples that were analyzed might be an explanation for inability to demonstrate statistical significance in the patient subsets.

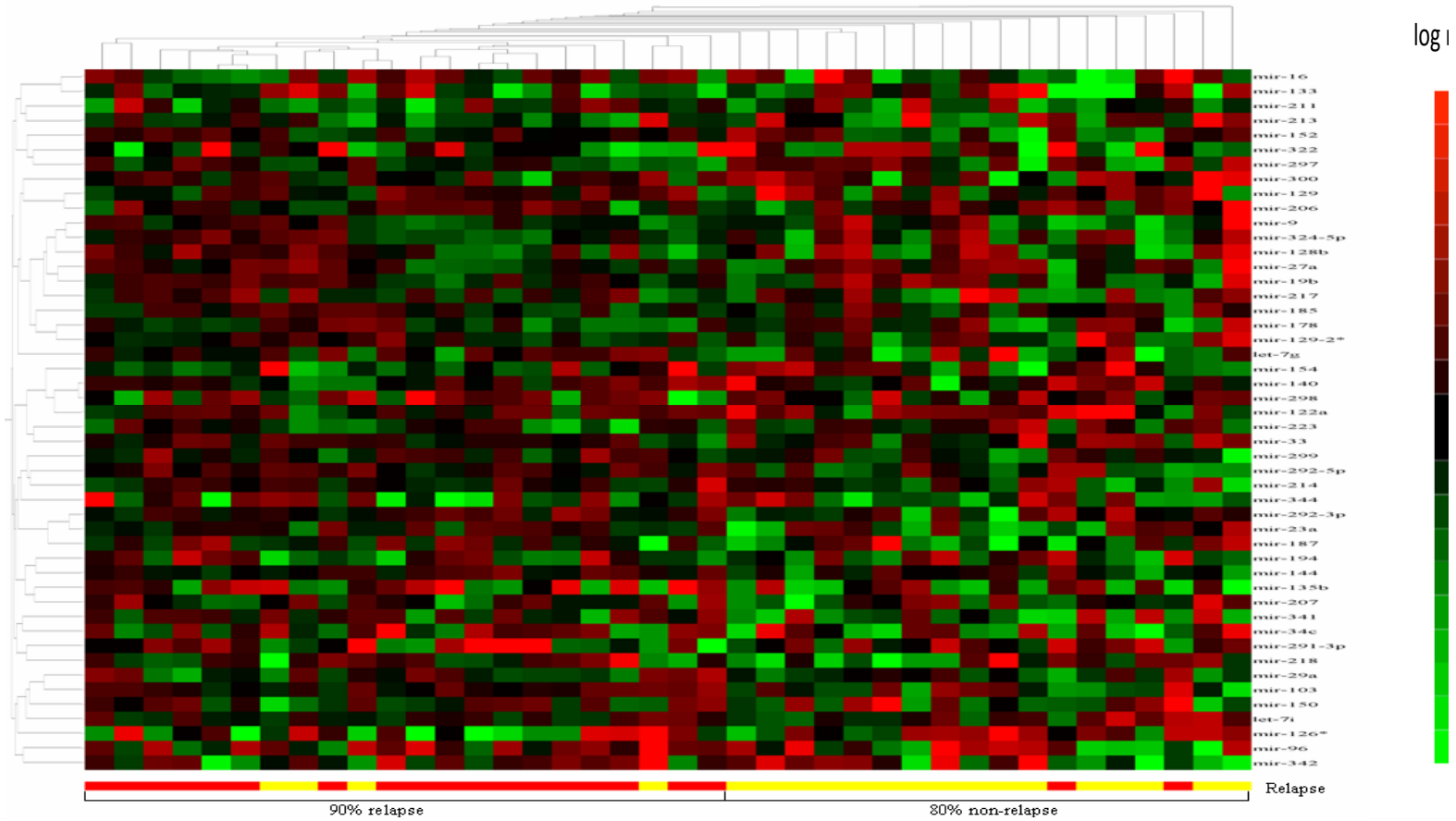

Figure 2.4: Endogenous miRNA Expression of 114 miRNAs in Prostate Cancer. 90% of patients in the chemical-relapsed subset were segregated according to heat map distance clustering, based on the expression profile of 48 miRNAs. This hierarchical cluster analysis excluded 80% of non-relapse patients. Clinical status of individual patients is indicated by color on X axis (red, chemical-relapse, yellow, non-relapse patients). Patients are represented in the X-axis and are sorted using the Euclidean distance metrics. T/N ratios of miRNAs are represent in the Y-axis and are clustered using hierarchical clustering with standard correlation.

Table 2.4: Differential miRNA Expression in Chemical Relapse and Non-relapse Prostate Cancers by mirMASA

miRNAs	Mean T/N Ration (SD)		Ratio
	Relapse	Non-relapse	(Relapse/Non-relapse)
Reduced expression in patients with chemical relapse			
miR-342	1.01 (0.08)	2.11 (3.48)	0.48
miR-154	0.99 (0.12)	1.50 (1.63)	0.66
miR-140	1.02 (0.06)	1.29 (1.12)	0.79
miR-298	1.02 (0.11)	1.27 (0.97)	0.81
miR-129	1.03 (0.11)	1.27 (0.74)	0.83
miR-126	1.01 (0.25)	1.15 (0.37)	0.88
miR-122a	1.02 (0.07)	1.09 (0.18)	0.94
miR-213	0.97 (0.06)	1.03 (0.18)	0.94
miR-300	0.99 (0.05)	1.04 (0.10)	0.95
Increased expression in patients with chemical relapse			
miR-135b	1.29 (0.70)	1.12 (1.11)	1.14
miR-23a	1.01 (0.04)	0.93 (0.21)	1.08
miR-34c	1.01 (0.09)	0.94 (0.30)	1.07
miR194	1.03 (0.11)	0.96 (0.08)	1.07
miR-218	1.02 (0.08)	0.96 (0.13)	1.06
miR-96	1.05 (0.09)	0.99 (0.34)	1.06
miR-16	1.02 (0.10)	0.97 (0.18)	1.06

Discussion

Currently, data regarding the miRNA expression profile in prostate cancers is limited. In this study, we compared the differential miRNA expression of early-stage prostate cancer patients using a paired analytical approach. We used a high-throughput liquid-phase bead-based hybridization method, similar to that of Lu et al. (Lu, Getz et al. 2005), who were the first to use this method to classify and define miRNA profiling in human lung cancer. Comparing to solid-phased array-based analyses, liquid-phase hybridization may be more sensitive in discriminating modest changes in miRNA expressions (Lu, Getz et al. 2005; Barad, Meiri et al. 2004). Although the differential

expression of coding mRNA in normal and malignant tissues may be differ in order of magnitude, smaller 1 to 2-fold differences in miRNA expressions is commonly seen (Xi, Shalgi et al. 2006; Rana 2007; Coller, Forman et al. 2007). Taking these into consideration, together with unique technical features of our analysis, may explain the modest T/N ratios observed in our study.

Ozen et al investigated the expression 480 miRNAs in 10 benign peripheral zone tissues and 16 prostate cancer tissues from radical prostatectomies using miRNA microarray technology (Ozen, Creighton et al. 2007). A total of 85 miRNAs were found to be detectable in normal and/or neoplastic prostate tissue. Most of the miRNAs detected were downregulated, 76 out of the 85 were significantly downregulated. They discovered these miRNAs to be significantly downregulated, let-7 family (7b-g, 7i), miR-26a-b, miR-29a-c, miR-30a-e, miR-99a-b, miR-125a-b, and miR-200a-b (Ozen, Creighton et al. 2007). In a recent study, we have investigated the expression of 114 miRNAs in 40 maglinant patient samples and found 5 miRNAs that consistently and significantly downregulated in tumor tissue comparing to their adjacent normal tissue. These 5 include miR-23b, miR-100, miR-145, miR-221, and miR-222, with miR-143 approaching significance (Tong, Fulgham et al. 2008). Our results confirm the findings of Lu and Volinia in the observation of downregulated miR-143, and miR-145 in prostate cancers (Lu, Getz et al. 2005; Volinia, Calin et al. 2006).

During the micro-dissection process, it is inevitable that the dissected normal tissue might contain hyperplastic/premalignant areas, or the malignant dissection incorporating non-malignant tissue may contribute to a less profound change, as reflected in a less remarkable reduced T/N ratio. To take into consideration the intersample variations, 5S

RNA hybridization was performed in parallel and used to normalize the patient T/N ratios. In numerous transformed and tumor cell types, elevated expression of RNA polymerase III activity has been observed, which might in turn elevate the expression of essential untranslated transcripts such as 5S rRNA (White 2004). However, 5S RNA expression did not alter significantly between normal and malignant tissue when examined across all patient samples.

Using the paired analytical approach, we identified five miRNAs (miR-23b, -100, -145, -221, and -222) that were significantly downregulated by both the statistical tests, SAM and paired *t*-test with Bonferroni corrections. Quantitative real-time PCR (qPCR), using primer/probe sets that were designed to exclude precursor miRNAs, was used to confirm the downregulation of the five identified miRNAs. It is advantageous to only analyze mature miRNAs as studies have shown that precursor expression does not necessary translate to mature miRNA presentation. qPCR analyses confirmed mirMASA findings that miR-23b, -100, -145, -221 and -222 were downregulated. We also found that miR-100 had decreased expression that approached significance using the previously mentioned analysis criteria. The validity of our findings is indirectly supported by the collateral downregulation of miR-221 with miR-222, and miR-143 with miR-145, which are encoded as clusters.

In comparing miR-100 findings by the two techniques, qPCR analyses confirmed that four of the eight patients exhibited a reduced miR-100 expression by $\geq$ 20% in malignant tissues (Table 2.4). These findings support the premise that mirMASA's may be more sensitive for discriminating differential miRNA expression (van Rooij, Olsen et al. 2007).

Several recent studies on prostate cancer miRNA phenotypes that were based on limited sample size support our miRNA observations. Mattie et al examined fine needle aspirations and primary needle core biopsies of metastatic lesions and found 46 miRNAs that defined the prostate cancer miRNA signature in their study, which included the decreased expression of miR-23b, -100, -143, -145 and -222, as well as miR-100 (Mattie, Benz et al. 2006). Our observation of decreased miR-143, -145, -221 and -222 in Stage T2a/b prostate cancer specimens was among the 22 miRNAs that Porkka et al. found to be decreased in five untreated and four hormone-refractory prostate carcinomas using a array-based hybridization analysis (Porkka, Pfeiffer et al. 2007). In a similar study of prostate cancer cell lines, miR-221 and -222 were found to be downregulated in more aggressively growing in the prostate cancer cell line PC-3 as compared to the slower cell lines LNCaP and 22Rv1. Our observation of decreased miR-145 expression in malignant cancer tissue was consistent with Ozen et al.'s recent report that miR-145 was one of the most frequently downregulated miRNAs in 16 prostatecomy samples from patients with or without chemical-relapse (Ozen, Creighton et al. 2008).

These studies, in conjunction with our work, demonstrate the differential expression of miRNAs among normal and malignant cells from the same patient, indicating that altered miRNA activity may accompany prostate oncogenesis. Further, differences in miRNA expression were also observed between patients with chemical relapse vs the non-relapse group. Our initial findings with limited number of patients in chemical relapse and non-relapse subset suggest that additional analysis, with a more robust population sample size,may identify unique miRNA phenotypes for early relapse prostate cancer. Despite by miRNA profile, further, indepth analysis is needed to determine its

clinical relevance. The remaining part of my dissertation will focus on select dysregulated miRNAs.

CHAPTER THREE

Growth Inhibition Properties of MicroRNAs

Previously, we have shown that the introduction of a small-interfering RNA (siRNA), was able to silence mutant K-ras overexpression in non-small cell lung cancer (NSCLC) yielding growth inhibition as well as K-ras mRNA and protein knockdown (Zhang, Nemunaitis et al. 2006b). Similarly, through ectopic expression of down-regulated miRNAs, cancer cell growth inhibition can be achieved if the miRNA target genes that are necessary for cancer proliferation. This growth inhibitor effect of miRNA was also shown by the transient expression of precursor miR-143 and -145 inhibited the growth colon cancer cells (Akao, Nakagawa et al. 2006). Based on these findings, we examined the growth modulatory activity by reconstitutive studies using miRNAs that were previously shown to be downregulated in prostate cancer patients.

In the previous chapter, we examined the use of a high-throughput liquid phase bead-based hybridized to investigate dysregulated miRNAs in 40 prostatectomy patients. We saw a differential expression pattern when malignant tissue was compared to its tumor counterpart. Our findings of consistently decreased expression of five miRNAs (miR-23b, -100, -145, -221, and -222) are indirect evidence that these miRNAs may be involved in prostate cancer pathophysiology. To better understand the roles of these dysregulated miRNAs in prostate cancers, reconstitutive studies were carried out to explore their effects on prostate cancer cell growth.

Of the five downregulated miRNAs, we selected 3 miRNAs (miR-23b, -145 and -222) to further characterize their involvement in prostate cancer cell growth regulation, using the trypan blue exclusion and MTT cell proliferation assays. In this study, we examine the hypothesis that downregulated miRNAs have an impact in the pathophysiology of prostate cancer by altering cell growth. We hypothesize that transient expression of downregulated miRNAs can induce growth inhibition. miR-100 was not studied since its significant downregulation cannot be confirmed independently by qPCR analysis. Reconstitution with miR-221 was not carried out in view of the expected overlapping targeting activity with miR-222 (Lim, Lau et al. 2005; Bandres, Cubedo et al 2006; Rana 2007). The ectopic expression of down regulated miRNAs namely, miR-23b, miR-145, miR-222, was examined separately or in combination in equimolar concentrations for their ability to modulate LNCaP prostate cancer cell growth. The prostate cancer line LNCaP displayed a similar phenotype of reduced expression of miR-23b, -145, -221, and -222, and increased miR-141; and thus was selected for reconstitution studies.

Material and Methods

Cell Lines

The prostate carcinoma cell line LNCaP (clone FGC) was obtained from the American Type Culture Collection (ATCC, Manassa, VA). This cell line was maintained and cultured in RPMI 1640 Medium (modified to contain 2mM L-glutamine, 10mM HEPES, 1mM sodium pyruvate, 4500 mg/L glucose, and 1500 mg/L

sodium bicarbonate, Cat# 30-2001, ATCC, Manassa, VA) with 10% fetal bovine serum (FBS; Atlanta Biologicals, Atlanta, GA).

Cell Viability Assays

For determination of the growth inhibitory affect effect of miRNAs, target cells (4.5×10^4) suspended in medium were seeded into 24-well plates, and transfected with predesigned (predetermined mature miRNA sequences), synthetic miRNA (50nM, miRIDIANS; Dharmacon, Chicago, IL) using reverse transfection (cells and transfection agents are mixed together before seeding into culture plates) lipofection according to manufacturer's recommendation (siPORT *NeoFX* Transfection Reagent; Ambion, Austin TX). To determine transfection efficiency, a plasmid containing a GFP reporter gene (gWiz-GFP plasmid; Aldevron, Fargo, ND) was transfected in parallel. The total of fluorescent cells were divided by the total number of viable cells. The Trypan blue exclusion assay was used to determine cell viability in triplicates (please see Appendix for attached protocol). To ensure that the enumeration process is unbiased, the total and viable cell counts in a hemacytometer chamber was performed by two independent observers by light microscopy. Controls include untreated cells (UNT), cells treated with transfection reagent only (Mock), and cells transfected with scrambled miRNA (Negative miRNA).

Confirmation studies were done by the MTT assay which measures mitochondrial activity. MTT assay was performed according to the manufacturer's recommendation (TACS MTT Cell Proliferation Assay, R&D Systems, Minneapolis, MN). 1.0×10^4 cells into 96-well plates and transfected by reverse transfection with 50nM of synthetic miRNA. A standard curve was established by serial diluting cells

from 1.0 x 10^3 to 1.28 x 10^5 cells per well and seeded in parallel. After 48 hours post-transfection, 10 μL of MTT (3-[4,5-dimethlythiazol-2-yl]-2, 5-diphenyltetrazolium bromide; TACS MTT Assay, R&D Systems, Minneapolis, MN) was added to each well and incubated overnight. On the next day, 100 μL of detergent was added and incubated in dark for 2 hours at room temperature. The colormetric reaction was quantified using spectrophotometer measurements at 570 nm with a reference wavelength of 690 nm (SpectraMax 340, Molecular Devices, Sunnyvale, CA).

Results

Growth Inhibitory Effects of Down Regulated miRNA Reconstitution

To characterize the pathophysiological implication of downregulated miRNA expression, synthetic miRNAs having the same target mRNA specificty were used to determine whether their reconstitution impacted cell growth. Multiple prostate cancer lines were phenotypically analyzed to validate the miRNA expression pattern as compared with patient specimens. The LNCaP line displayed a similar phenotype of reduced expression of miR-23b, -145, -221 and -222, and increased miR-141 (Table 3.1). LNCaP cells were transfected with oligonucleotides constructs that correspond to the mature sequence of each miRNA. The growth inhibitory effect of down regulated miRNA reconstitution in LNCaP cancer cells was time dependent from 24 hours to 72 hours, with its effect plateauing at 48 hours post-transfection. The LNCaP cell growth reduction was also dependent on transfecting miRNA dose, with growth reductions of 15% at 12.5 nM, 24% at 25 nM, and 36% ($p < 0.05$, Student's two-tailed t-test, $n = 3$ per dose) at 50 nM following miR-222 transfection compared to negative miRNA

treatment. An optimal dose of 50 nM was selected for further experiments as increasing the dose to 100 nM did not substantially promote the growth inhibitory effect.

Table 3.1: miRNA Expression in LNCaP Cell Line

	miRNA Expression			
	Expression level (fg)[a]		Normalized MFI ($x10^3$)[b]	
miRNA tested	LNCaP	Non-malignant	LNCaP	Non-malignant[c]
23b	0.69	10.5	13.0	92.1
145	0.16	87.3	6.9	62.8
221	NT	NT	18.0	131.5
222	6.5	94.6	18.8	69.5
141	120	49.2	137	86.8

[a]Determined by qRT-PCR analyses. Values represent mean of triplicate determinations. LNCaP and a single non-malignant prostate specimen was harvested following the OCT fixation process. NT: not-tested.

[b]MFI values were normalized to 5S RNA readouts following mirMASA analysis. LNCaP cells were subjected to formalin fixation and paraffin embedding (FFPE) prior to RNA extraction, to achieve proper comparison with simiarly treated non-malignant prostate specimens.
[c]Mean of 40 samples.

Cultures treated with negative miRNA did not differ significantly from untreated control (109% of untreated culture, $p > 0.05$). Ectopic expression of miR-23b, -145, and -222 significantly inhibited LNCaP growth by 38%, 32%, and 37% respectively at 24 hours post-transfection (Figure 3), as compared with negative miRNA treated culture ($p < 0.01$, Student's two-tailed t test, $n = 3$ per miRNA). This level of growth inhibition compared favorably with a transfection efficiency of 40.8 $\pm$ 5.4 %, as determined by reporter gene (gWiz-GFP plasmid) analysis. Reconstitution with miR-221 was not carried out in view of the expected overlapping targeting activity with miR-222 (Lim, Lau et al. 2005; Bandres, Cubedo et al 2006; Rana 2007). In contrast,

reconstitution with miR-141, which was upregulated in LNCaP and in 75% of patient samples, did not significantly alter the growth of LNCaP cells (<5% growth inhibition, $p > 0.05$ as compared with negative miRNA transfected cells; Figure 3.1). Similarly, mock transfection, or treatment with cel-miR-67 (*C. elegans* miRNA with minimal sequence identity with human miRNAs) did not significantly impact LNCaP growth.

Interestingly, combined treatment with equimolar (16.6nM, each) concentrations of miR-23b, -145, and -222 did not generate a synergistic inhibitory response (39 % growth inhibition as compared with negative miRNA treatment, Figure 3.1). The effective dose to achieve 50% growth inhibition (ED_{50}) for miR-23b, miR-145, and miR-222 was 84.5 nM, 52.8 nM, and 75 nM, respectively, according to dose response studies, as compared with the molar equivalent of 55.9 nM in the combined treatment of all 3 miRNAs. The capacity to inhibit prostate cancer cell growth through transient expression is suggestive of a growth regulatory role for the downregulated miRNAs in prostate oncogenesis. This reconstitutive approach may serve as a viable experimental therapeutic approach for human prostate cancer.

The MTT (3-[4,5-dimethlythiazol-2-yl]-2, 5-diphenyltetrazolium bromide) assay measures mitochondria metabolic activity and is commonly used for the monitoring of cell culture metabolism. With the use of the MTT assay, cells treated with miR-145 showed a maximum growth inhibition of 20% ($p < 0.05$, Student's two-tailed t-test, $n = 6$) as compared to negative miRNA treatment 4 days post-transfection (Figure 3.2). These findings confirm that miR-145 had a growth inhibitory in LNCaP prostate cancer cells. Statistical analysis (Student's two-tailed t-test) showed no significant difference in growth inhibition between mock, negative miRNA, whereas cells treated

with miR-145 exhibited significant growth inhibition. In this experiment, we only examined the growth inhibitory effect of miR-145 by the MTT assay to represent the effectiveness of downregulated miRNAs in growth inhibition.

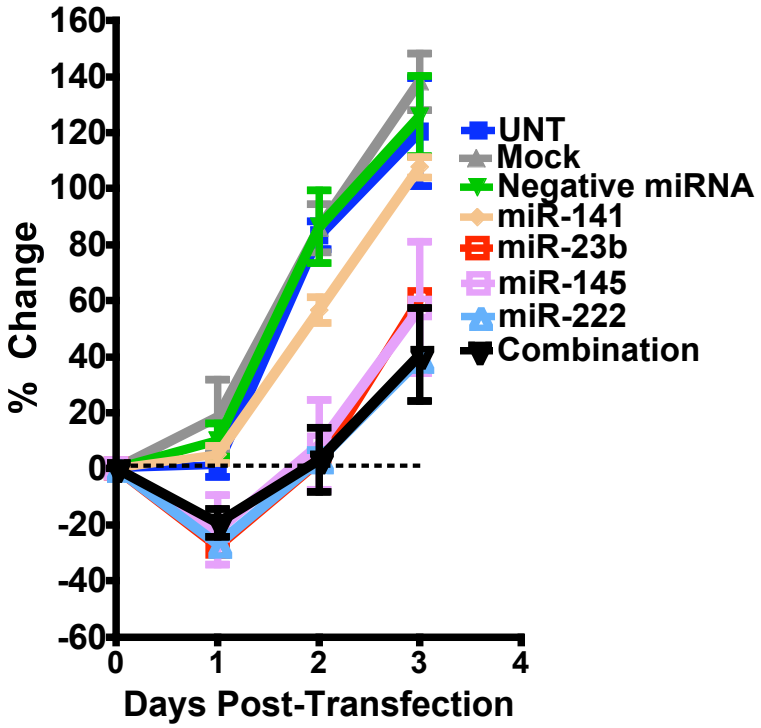

Figure 3.1: miRNA Reconstitution Effect on Prostate Cancer Cell Growth. LNCaP were treated with 50 nM of miRNAs or mock-transfected (only transfection reagent without any miRNA). Values are represented as the % change in viable cell numbers (mean ± S.D.) compared to the initial seeded cells at Day 0. Combined treatment was carried out with pooled eqimolar concentration of miR-23b, -145 and -222 with a total concentration of 50 nM of miRNA.

Discussion

In this study, we found that introduction of downregulated miRNAs (miR-23b, -145, and -222) effectively decreased LNCaP cell growth whereas introduction of the upregulated miR-141 did not alter growth. The ability to inhibit prostate cancer cell growth through the transient expression of downregulated miRNAs suggests its'

growth regulatory role in prostate oncogenesis. Combined treatment of equimolar of 3 downregulated miRNAs did not enhance the growth inhibitory effect compared to single oligonucleotide miRNA dose suggest that these dysregulated miRNAs might target genes of overlapping pathways. Currently, we are the first to demonstrate growth inhibitory effects of ectopic expressed dysregulated miRNAs in prostate cancer cells. Other research has shown similar growth inhibitory effects of miR-145 in other cancers.

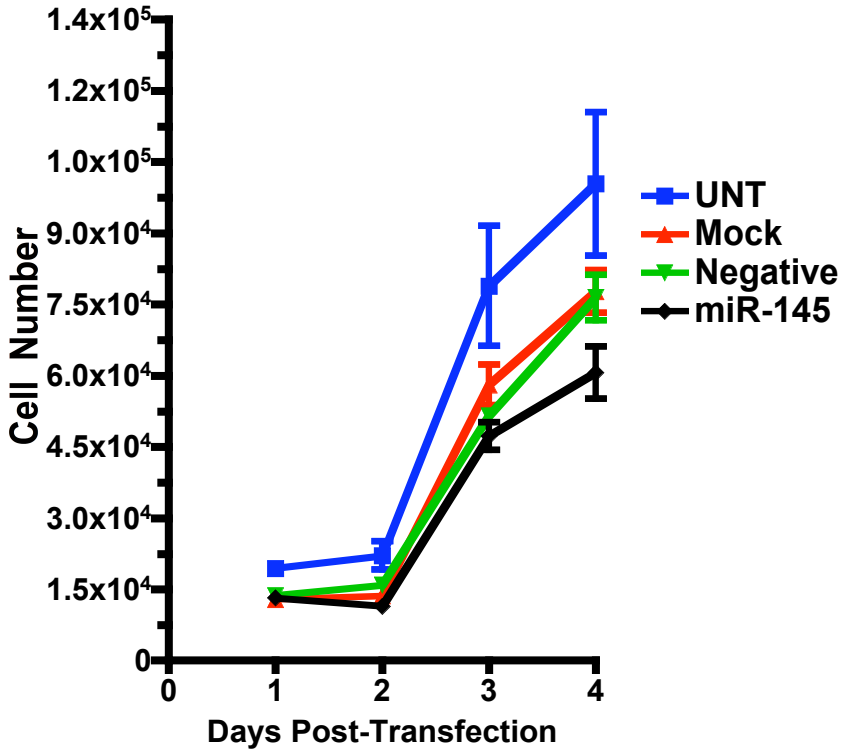

Figure 3.2: miR-145 Reconstitution Effect on Prostate Cancer Cell Growth. LNCaP cells were treated with 50 nM of miR-145. Growth was measured as a function of mitochondria activity. Maximum growth inhibition by miR-145 was observed on Day 4 post-transfection.

Akao and colleagues also found that the expression levels of both miR-143 and -145 were significantly decreased in B-cell malignancies by qPCR analysis. Through

the exogenous expression of either precursor or mature miRNAs, miR-143 and -145, negatively impacted cell growth in B-cell malignant culture in a dose dependent manner (Akao, Nakagawa et al. 2007). This observation of miR-145 effect on growth inhibition mirrors our findings although we achieved a higher degree of growth inhibition

Several groups have previously reported the downregulation of miR-143 and -145 were downregulated in other solid tumors. At the time of writing this dissertation, we were the first group to study the effects of miR-145 on prostate cancer cell growth. Michael et al. were the first to publish that there was an overall decrease in miRNA expression in several cancer types including colorectal adenocarcinoma when compared to normal mucosa, and both miR-143 and -145 were consistently reduced in adenomatous and cancer stages of colorectal cancer (Michael, O'Connor et al. 2003). Later, Bandres et al. used qPCR to examine 16 colorectal cancer cell lines and 12 matched pairs of non-malignant and malignant patient tissues, and found 13 miRNAs with altered expression, including miR-145 (Bandres, Cubedo et al. 2006). Also using qPCR, Akao et al. found that miR-143 and -145 were decreased in colorectal cancers, and further investigated in their growth inhibition activity in human colon cancer cell lines (Akao, Nakagawa et al. 2007). They found that precursor miRNAs miR-143 and -145 inhibited cell growth in a dose-dependent manner. These results suggest a growth regulatory role for miR-145 as a potential therapeutic treatment in colorectal cancers.

To explore the physiologic relevance of miRNAs that were downregulated, we found that ectopic expression of miR-23b, -145, and -222 led to decreased growth in LNCaP cells. It is likely that this decrease in cell numbers is a cause of cell death as

counted by trypan blue. This preliminary finding suggests that lowered expression of select miRNAs likely impact the growth and/or survival of the prostate cancer cells. We are the first to report that through the ectopic expression of miR-23b, -145 and -222 led to decreased growth in prostate cancer cells.

It is of interest to note that combined treatment with all 3 miRNAs did not generate a synergistic inhibitory effect. The possibility exists that loss of function from these regulatory molecules impacts a common, or overlapping regulatory pathways that may be pivotal for prostate cancer cell growth. The absence of an additive effect may also be attributable to the presence of a predominant, mRNA target for which the cancer cell is oncogenically addicted (Weinstein 2002).

CHAPTER FOUR

Target Prediction and Validation of miRNAs

Studies described in Chapter 2 and 3, showed that miR-145 was one of the most significantly downregulated miRNAs in prostate cancer. This miRNA reduced LNCaP growth by 32% when introduced *in vitro*, ectopically. We have designed studies to identify potential gene targets for miR-145. Our strategy involves first using cDNA hybridization array analysis to identify abnormally expressed genes, that fell within the roster of miR-145-predicted targets *in silico.* The endogenous expression of gene candidates from this reduced list of possible targets was determined by qPCR before and after reconstitution with miR-145. Further, a reporter gene system comprising of the cloned 3' UTRs (untranslated region) of the target sequence was used to investigate the binding and confirmation of miR-145 targeting.

Many programs and *in silico* algorithms are available for miRNA target prediction. Each program uses different algorithms, based on the binding affinity, conformational folding and other properties. The differences and similarities of these algorithms are described in the Discussion section. We feel that the best strategy is to use at least two to improve target prediction accuracy. In our *in silico* analysis, we first used the online tool TargetScan (http://www.targetscan.org/) to determine possible targets of miR-145. Once these targets were established, we confirmed the targets using another online tool miRanda (http://www.microrna.org/). We elected to use these two online tools based on their popularity as well as their easy to use user

interface. These miR-145 targets were then cross referenced to our high throughput, gene microarray data for LNCaP to reveal candidate genes that were upregulated in the miR-145 downregulated cell line. This screening process allows us to identify a limited number of gene targets that warrants further investigation.

Table 4.1 has a list of current programs best suited to identify miRNA targets in mammalians.

Table 4.1: Available Programs for miRNA Target Predictions

Reference	Program Name	Website	Organism
Lewis et al. 2003 Lewis et al. 2005	TargetScan TargetScan S	http://www.targetscan.org/archieves.html http://genes.mit.edu/tscan/targetscanS2005.html http://www.targetscan.org/ (Current Version)	Mammals
Enright et al. 2003 John et al. 2004	miRanda	http://www.microrna.org/	Fruit Fly Mammals
Rehmsmeier et al. 2004	RNAhybrid	http://bibiserv.techfak.uni-bielefeld.de/rnahybrid/	Any
Kiriakidou et al. 2004	DIANA-microT	http://diana.pcbi.upenn.edu/cgi-bin/micro_t.cgi	Any
Rusinov et al. 2005	MicroInspector	http://mirna.imbb.forth.gr/microinspector/	Any
Grun et al. 2005 Krek et al. 2005 Lall et al. 2006	PicTar	http://pictar.bio.nyu.edu/	Fruit Fly Mammals Any

Programs listed are those that are suited for Mammals.

Figure 4.1 is a flow-chart that summarizes our experimental design for determining and confirming miRNA targeting. In this study, we examine the direct binding of miR-145 to 3' UTR regions of *in silico* predicted targets. We hypothesize that miR-145 binds directly to the predicted target PTGFR and silences its expression.

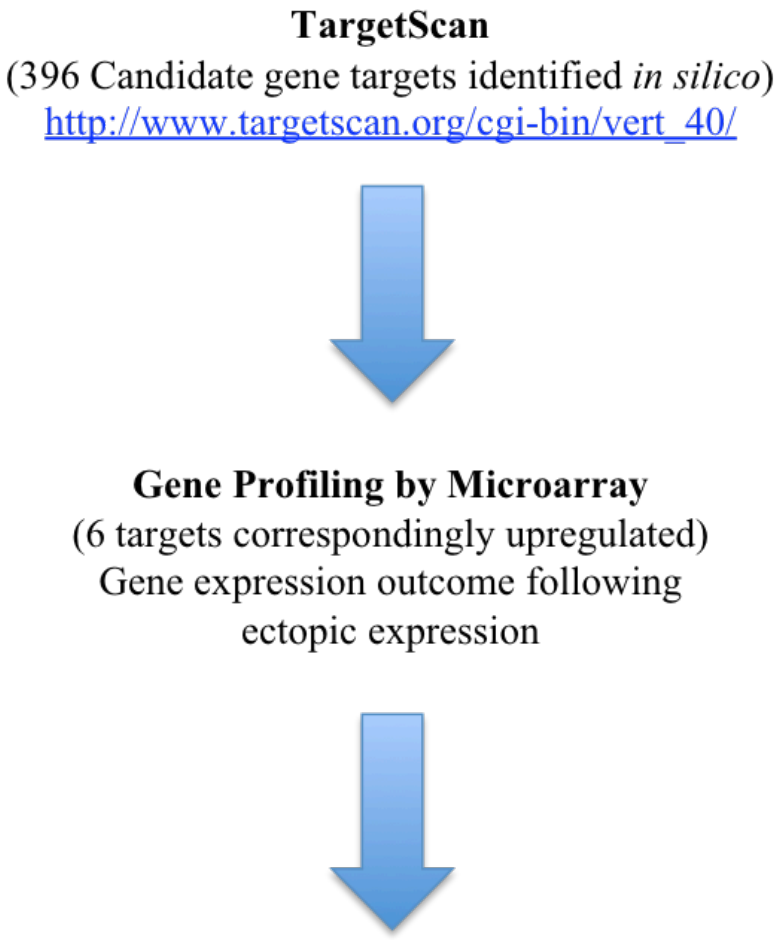

Figure 4.1: miR-145 Target Identification. By cross referencing the *in silico* target search for miR-145 with the target gene profiling analysis by microarray, we can identify mRNA targets that are upregulated in LNCaP cells with decreased miR-145 expression. The endogenous expression of gene candidates from this reduced list of possible targets was determined by qPCR before and after reconstitution with miR-145. The 3' UTR of candidate genes containing the miR-145 targeting sequence are cloned into a luciferase expression plasmid to be used for miR-145 target binding validation.

Material and Methods

Cell Lines

The prostate carcinoma cell lines LNCaP (clone FGC), 22Rv1, Du-145, PC-3, and normal prostate epithelial RWPE-1 were obtained from the American Type Culture Collection (ATCC, Manassa, VA). The cell lines LNCaP, 22Rv1, and Du-145 were maintained and cultured in RPMI 1640 Medium (modified to contain 2mM L-glutamine, 10mM HEPES, 1mM sodium pyruvate, 4500 mg/L glucose, and 1500 mg/L sodium bicarbonate, Cat# 30-2001, ATCC, Manassa, VA) with 10% fetal bovine serum (FBS; Atlanta Biologicals, Atlanta, GA). PC-3 was cultured in F12K (Kaighn's Modification of Ham's F-12 Medium, Cat# 30-2004, ATCC, Manassa, VA) supplemented with 10% FBS. The normal prostate epithelial cell line RWPE-1 was cultured in Keratinocyte media supplemented with 0.05 mg/mL fetal bovine pituitary extract (BPE) and 5 ng/mL human recombinant epidermal growth factor (EGF) (Keratinocyte Serum free media Kit, Cat# 17005-042, Invitrogen, Carlsbrad, CA).

cDNA Microarray Analysis

Total RNA was isolated using the RNeasy kit (Qiagen, Valencia, CA).The RNA quality was determined by spectrophotometry 260/280 ratios (NanoDrop ND-1000, Thermo Fisher Scientific, Wilmington, DE) and integrity by electrophoresis using the BioRad Experion RNA StdSens Chip (BioRad, Hercules, CA). Gene expression profiles of each cell line was determined by hybridization with the Affymetrix Human Genome U133 Plus 2.0 oligonucleotide probe array (Affymetrix, Santa Clara, CA), according to standard protocols (Microarray Core Facility, UT Southwestern Medical

Center, Dallas, TX). cDNA is synthesized from 200 ng of extracted RNA. aRNA is then synthesized from cDNA with biotin labeled ribonucleotides. The aRNA is then fragmented and hybridized to Affymetrix Human Genome U133 Plus 2.0 GeneChip (Affymetrix, Santa Clara, CA). The hybridized GeneChips are then scanned and quantified. Please see Appendix for detailed protocol. Raw mRNA expression was than normalized and analyzed using the GeneSpring 7.3.1 software (Agilent Technologies, Santa Clara, CA) to identify mRNA transcripts that were differentially expressed between the different cell lines.

qPCR Confirmation of Microarray Analysis

100 ngs of extracted RNA was used for qPCR confirmation of microarray analysis. Quantitative real time PCR (qPCR) is divided into two major steps, 1) RNA reverse transcription, and 2) real time PCR using specific TaqMan Probes. The reverse transcription step (High Capacity cDNA Reverse Transcription Kit, Applied Biosystems, Foster City, CA) was preformed according to the manufacturer's protocol (25˚C for 10 mins, 37˚C for 120 mins, and 85˚C for 5 secs). The quantitative real time PCR was done using a PCR master mix containing AmpliTaq Gold DNA polymerase (TaqMan Universal PCR Master Mix without AmpErase, Applied Biosystems, Foster City, CA) and gene-specific amplification primers (TaqMan Assays, Applied Biosystems, Foster City, CA). The following mRNA expressions were confirmed by qRT-PCR: *PTGFR, RASSF2, MYCN,* and *CCND2* according to the manufacturer's protocol (95˚C for 10 mins, 40 cycles: 95˚C for 15 sec, 60˚C for 60 sec, Applied Biosystem). *GAPDH* was detected in parallel and used as a loading normlization.

mRNA Knockdown by miR-145 in LNCaP Cells

At 24 hours before transfection, LNCaP or 22Rv1 cells were seeded into 24-well plates at 2 x 10^6 cells/well. Cells were treated with 25, 50, or 100 nM of miR-145 (Dharmacon, Chicago, IL) using 1 μL of transfection reagent (Lipofectamine 2000, Invitrogen, Carlsbrad, CA), according to manufacturer's protocol in a 24 well plate. At 48 hours post-transfection, cellular RNA was extracted and qPCR was performed to examine mRNA expression in miRNA-treated cultures. The same qPCR protocol was used as previously done for microarray analysis confirmation.

3' UTR Insertion into Luciferase Plasmid

Molecular cloning was performed using PCR amplification of target gene sequences (ref). The following primers were used for 3' UTR extraction from genomic DNA, PTGFR forward: gtggagtgcatgtcatcagc; PTGFR reverse: gctgcattaagatgttctctgg; RASSF2 forward: ctcagctcactgcaacatcc; RASSF2 reverse: acagcttgtgcatcttgtgc by PCR (GoTaq, Promega, Madison, WI) based on the following PCR conditions: 94˚C for 1 min; 35 cycles: 94˚C for 1 min, 48˚C for 30 secs, 72˚C for 30 secs; 72˚C for 9 mins. Gel electrophoresis was used to separate the PCR products, and gel bands of the appropriate molecular size were excised (PTGFR: 460 bp; RASSF2: 1100bp; Qiaquick Gel Extraction Kit, Qiagen, Valencia, CA). 1 μL of genomic DNA PCR product was then used as the template for cloning site (5' site to contain Xho I, and 3' site Not I) insert using the following PCR primers under same PCR conditions (PTGFR forward: ctcgaggtggagtgcatgtcatcagc; PTGFR reverse: gcggccgcgctgcattaagatgttctctgg; RASSF2 forward: ctcgaggctcagctcactgcaacatcc; RASSF2 reverse: gcggccgcacagcttgtgcatcttgtgc; underlined sequences denotes the

cloning sites). PCR products of the appropriate molecular size were excised and purified by 0.8% agarose gel electroploration (Invitrogen, Carlsbad, CA).

The luciferase plasmid psi-Check 2 (psi-Check 2, Promega, Madison, WI) was then digested using Xho I and Not I (Promega, Madison, WI), purified by 0.8% gel electrophoresis before insertion of the extracted PTGFR and RASSF2 3' UTRs with insertion sites. T4 DNA quick ligase (Quick Ligation Kit, New England BioLabs, Ipswich, MA) was used to ligate linearized psi-Check 2 and PTGFR or RASSF2 3' UTRs, according to manufacturer's protocol. The ligated products were propagated in *E.coli* competent cells (One Shot® Max Efficiency® DH5α™-T1R Competent Cells, Invitrogen, Carlsbrad, CA). The cloned plasmids were then extracted from the competent cell culture using the Purelink Quick Plasmid Miniprep Kit (Invitrogen, Carlsbrad, CA). Deoxyseqencing was performed to verify the clones (SeqWright, Houston, TX). The luciferase plasmids were named psi-PTGFR (psi-Check 2 with PTGFR 3' UTR insert), and psi-RASSF2 (psi-Check 2 with RASSF2 insert).

miR-145 Target Binding Assay

miR-145 can bind their 3' UTR sequence by cloning their miR-145 targeting sequence extracted from genomic DNA into a dual-luciferase reporter plasmid. The psi-Check 2 plasmid expresses two different luciferase genes (firefly and *Renilla*) that emit different wavelengths will be quantified. Firefly luciferase was expressed as a percent of *Renilla* luciferase to normalize plasmid loading. Transfection studies were carried out with LNCaP or 22Rv1 cells were seeded into 96 well white walled plates at 1×10^4 cells per well. At 24 hours after seeding, the cells were transfected using 1.0 µL of Lipofectamine 2000 (Invitrogen, Carlsbrad, CA), 1 µg of plasmid DNA, and

100 nmoles of synthetic miR-145 (miRIDIAN microRNA mimic, Dharmacon, Chicago, IL) per well. At 48 hours post-transfection, 75 µL of Dual-Glo Luciferase Reagent (Dual-Glo™ Luciferase Assay System, Promega, Madison, WI) was added. The culture was incubated for 10 mins at room temperature, and the firefly luminescence was quantified using a luminometer (DTX 880 Multimode Reader, Beckman Coulter, Fullerton, CA). 75 µL of Dual-Glo Stop & Go Regent (Dual-Glo™ Luciferase Assay System, Promega, Madison, WI) was added. The *Renilla* luciferase was then quantified after 10 mins of incubation. The results were then presented as the ratio of luminescence of the experimental reporter to luminescence from the control reporter. This normalized ratio for each well was compared to the untreated controls. The relative levels of fluorescence quenching were expressed as %RLU.

Results

Microarray Analysis of Dysregulated mRNAs in Prostate Cancer

The endogenous mRNA expression of the well known prostate adenocarcinoma, LNCaP (Figure 4.2) was compared with that of normal prostate epithelial cell line, RWPE-1. The genes were first prioritized by fold change (1.8 fold increased) when compared to RWPE-1. Eleven of these genes that were found to be upregulated in LNCaP cells have been cross-referenced as miR-145 putative targets (TargetScan; Table 4.2). The upregulated expression of 7, *PTGFR, PAK7, SRGAP-2, KIF3A, RASSF2, TGFBR2,* and *MYCN* was confirmed by repeat analysis in a second microarray experiment. Using a combination of *in silico* algorithms and gene array analysis, we narrowed down the possible gene targets of miR-145 to a more

manageable list. The upregulation of these genes may be related to the reduced expression of miR-145.

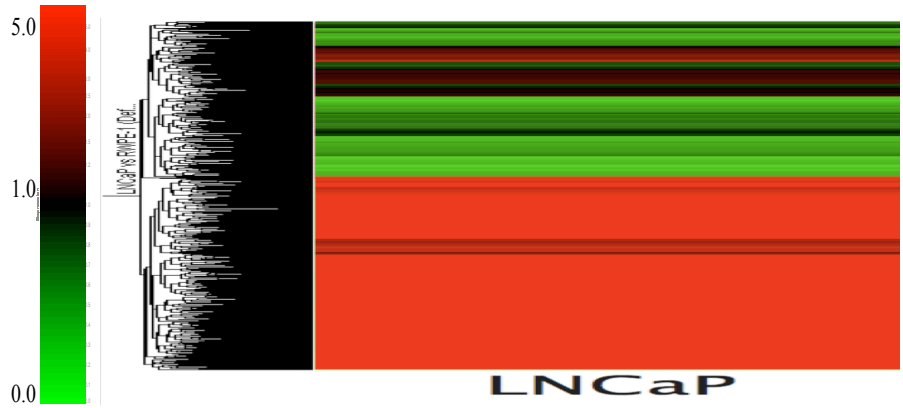

Figure 4.2: Heat Map of mRNA Expression in Prostate Cell Lines. Normal prostate epithelial cell line, RWPE-1, and prostate cancer cell line LNCaP were hybridized with the Affymetrix Human Genome U133 Plus 2.0 oligonucleotide probe array. LNCaP mRNA expression was normalized against against mRNA expression of RWPE-1. Genes were clustered using hierarchical clustering with standard correlation.

The genes that were selected for further investigation were based on their fold change, their relevance to prostate cancer, and qPCR kit availability. qPCR was performed to validate microarray findings of the increased expressions of *PTGFR, RASSF2, MYCN* and *CCND2* in the prostate cancer cell lines: LNCaP, 22Rv1, Du-145, and PC-3, as compared with the normal prostate epithelial cell line, RWPE-1. All 4 cell lines also expressed decreased expression of miR-145 when compared to RWPE-1 (Appendix H). *MYCN* was detected to be upregulated in the androgen sensitive cell lines LNCaP and 22Rv1, whereas *PTGFR* and *RASSF2* were upregulated in 3 of the 4 prostate cancer cell lines (Figure 4.3). The moderate increase in *CCND2* mRNA cannot be confirmed by qPCR among the 4 cell lines tested (1.2 fold increased compared to RWPE-1, Table 4.2). We also found that both MAP3K3 and MAP4K4

were not significantly upregulated in prostate cancer cells compared to RWPE-1. The increased expression of PTGFR and RASSF2 is suggestive of a causal relationship and warrants further investigation. The genes *PTGFR* and *RASSF2* were further selected for direct binding experiments using a luciferase reporter expression assay.

Table 4.2: Increased Expression of miR-145-Target Genes

Target Gene	Fold Difference (LNCaP/RWPE-1)	Putative Molecular Pathway
PTGFR	7.938	Ca^{2+} signaling
MAP3K3	4.942	MAPK signaling
MAP4K4	3.414	MAPK signaling
RASSF2	2.576	Regulate Ras
MYCN	1.331	Transcription Activation
CCND2	1.193	Cell Cycle
PAK7	6.631	ErbB signaling
APC	3.974	Apoptosis/Wnt signaling
SRGAP-2	3.818	Axon Guidance
KIF3A	2.614	Microtubule-associated motor
TGFBR2	1.473	MAPK signaling

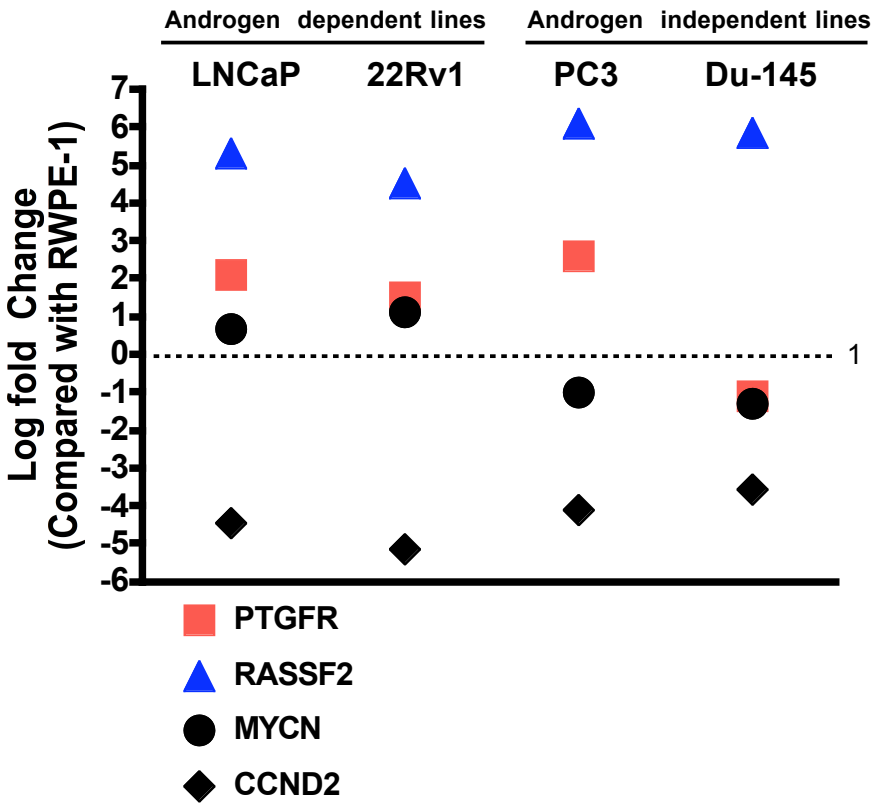

Figure 4.3: Target Gene Expression by qPCR in Prostate Cancer Cells as Compared to Normal Prostate Epithelial Cells, RWPE-1. qPCR analysis was performed using predesigned probes to confirm the increased expression of candidate genes.

PTGFR and RASSF2 Silencing by miR-145

To identify the interaction of miR-145 with *PTGFR* or *RASSF2* experimentally, we transfected the prostate cancer cell line LNCaP with a synthetic oligonucleotide corresponding to the mature miRNA sequence of miR-145. qPCR analysis was carried out to investigate the impact on *PTGFR* and *RASSF2*. At 24 hours post-transfection, *PTGFR* expression was significantly reduced by 26-30% at the mRNA level ($p < 0.003$, Student's t-test, $n = 5$) in miR-145 transfected cultures, as compared to scrambled miRNA treated cells. However, a dose dependent effect was no evident within the tested dose range of 25-100 nM (Figure 4.4). Thus increased miR-145

expression negatively impacted *PTGFR* transcripts. Neither Mock treatment of transfection reagent Lipofectamine 2000 only, nor a scrambled miRNA inhibited *PTGFR* expression (Figure 4.4A). miR-145 also significantly decreased *RASSF2* in LNCaP cells in a non-dose dependent manner. *RASSF2* was decreased by 42%, 45%, and 48% ($p < 0.0001$, Student's t-test, $n = 5$) when treated with 25 nM, 50 nM, or 100 nM, respectively (Figure 4.4B).

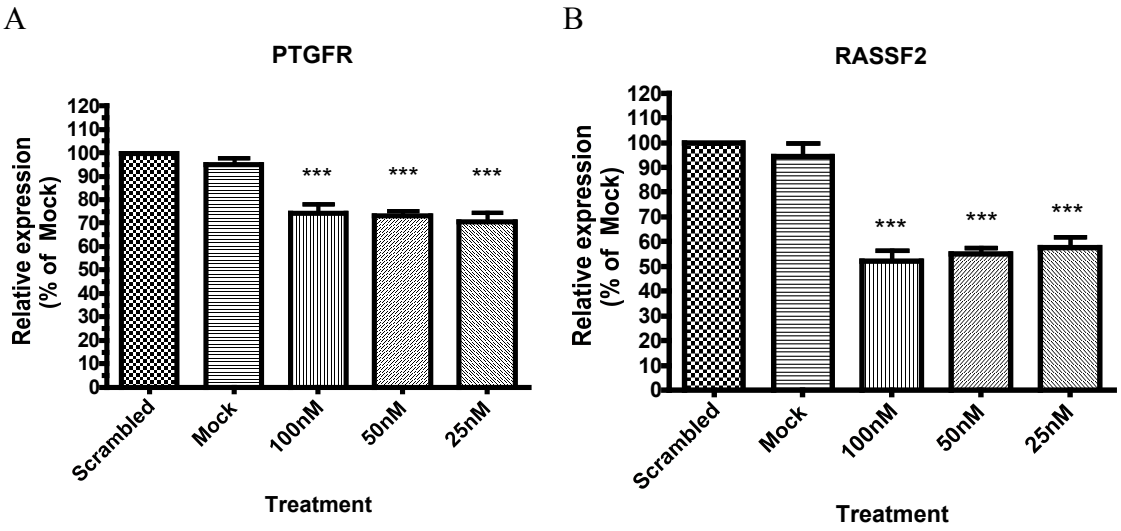

Figure 4.4: *PTGFR* and *RASSF2* expression 24 hours post miR-145 transfection in LNCaP cells. Each treatment RNA was isolated and quantified by qPCR. Results is expressed as relative expression compared to untreated (UNT) by the formula $2^{-\Delta\Delta Ct}$. PTGFR was downregulated by 30%, 27%, and 26%, and RASSF2 by 42%, 45%, and 48%, by 25nM, 50nM and 100nM of miR-145, respectively.

miR-145 Direct-Binding Assay

To validate miR-145 binding to its target genes, approximately 500 bp of the *PTGFR* and *RASSF2* 3' UTR containing the miR-145 targeting site was cloned and inserted into a dual-luciferase expressing plasmid (psi-Check 2). This gene reporter plasmid contains the expression of two luciferase genes, firefly and *Renilla,* where the expression of one is used to normalize loading. LNCaP and 22Rv1 cells were co-

transfected with the *PTGFR* or *RASSF2* 3' UTR containing luciferase plasmid (named psi-PTGFR and psi-RASSF2, respectively), and 100 nM of synthetic mature miR-145 oligonucleotides. Since the expression of firefly luciferase, used as loading control, was not significantly different in all treatments signifies that the viability of the cells does not play a role in the modulation of luciferase expression caused by miR-145. Scrambled miRNA treated culture did not significantly differ from untreated ($p > 0.05$, Student's t-test). At 48 hours post-transfection in LNCaP cells, miR-145 interacting with the PTGFR reporter vector, can be demonstrated by the reduction in luciferase expression compared to scrambled miRNA treatment (44%, $p = 0.0013$, Student's two-tailed *t*-test). Similarly, miR-145 cotransfection of 22Rv1 cells achieved significant reduction (20%, $p = 0.02$ Student's two-tailed *t*-test) of the psi-PTGFR expression (Figure 4.4C). Mock treatment did not significantly alter psi-PTGFR expression in either cell lines, LNCaP and 22Rv1, compared to scrambled miRNA treatment (Figure 4.5A and Figure 4.5C). miR-145 did not significantly reduce psi-RASSF2 expression when compared to untreated, mock, or scrambled miRNA in LNCaP treated cells ($p > 0.05$, Student's two-tailed *t*-test; Figure 4.5B). The level of psi-RASSF2 was not significantly decrease by mock, scrambled miRNA, or miR-145 in 22Rv1 48 hours post-transfection ($p > 0.05$, Student's two-tailed *t*-test; Figure 4.5D) although *RASSF2* mRNA was significantly down regulated by miRNA in our previous qPCR findings. In this study, we showed that miR-145 can interact with the 3' UTR of PTGFR and may modulate through this interaction.

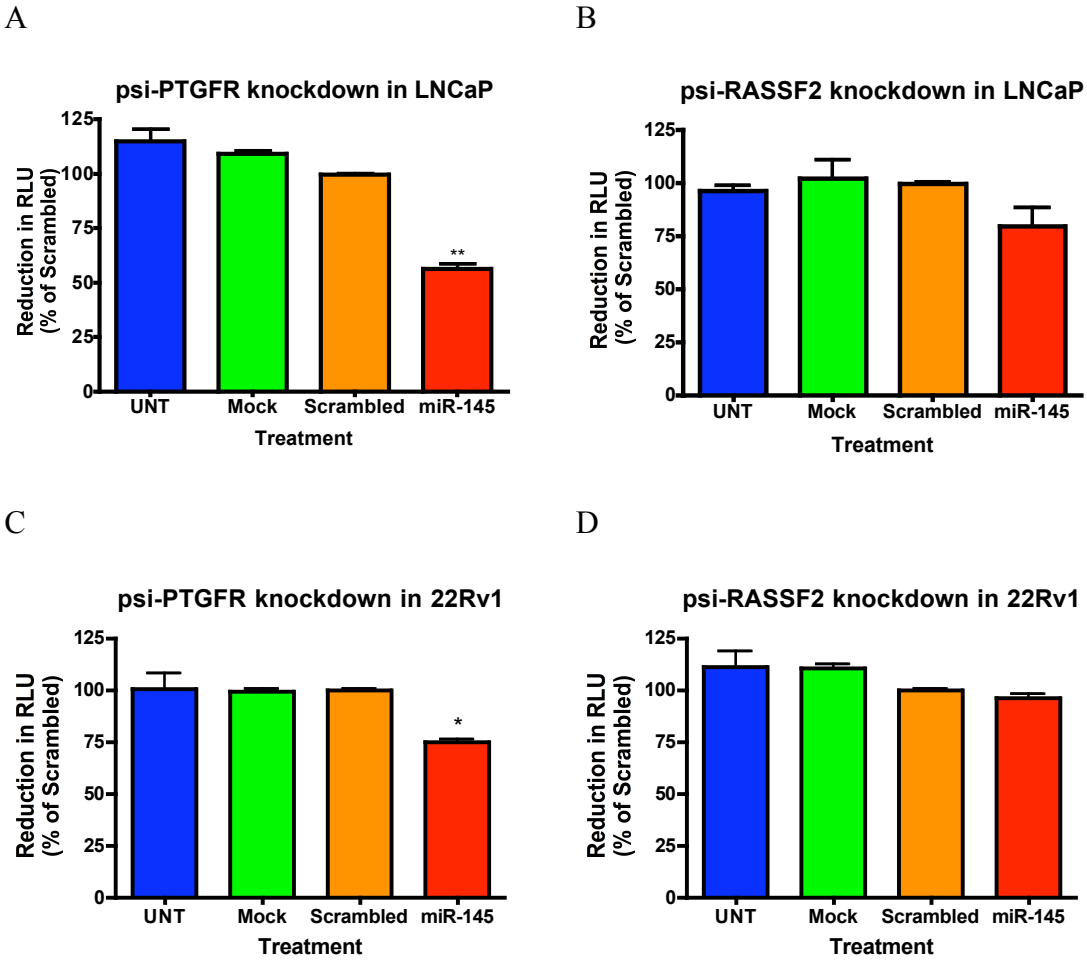

Figure 4.5: Luciferase reporter experiments in androgen dependent cell lines LNCaP and 22Rv1. LNCaP and 22Rv1 cells were seeded and co-transfected with psi-PTGFR or psi-RASSF2, and miR-145. Panels A and B are the results of LNCaP transfection, and 22Rv1 results are shown in Panels C and D. Firefly luciferase activity was quantified 48 hrs post-transfection. All treatments were compared to scrambled miRNA treated cultures and expressed as % of scrambled treatment.

Discussion

In this study, we examined up regulated mRNA expression in prostate cancer cell lines compared to a normal prostate epithelial. We also used *in silico* algorithms to predict possible miRNA targets based on their ability to bind the target's 3' UTR regions. Gene candidates of miR-145 regulation were called by combined analysis

with TargetScan and miRanda. With the multi-specificity of miRNAs current literature relies heavily on target prediction programs to identify potential target genes. Categorically, these miRNA target sites can be divided into: i) 5'-dominant canonical, these sites have perfect base-pairing to at least the seed portion of the 5' end of the miRNA and extensive base-pairing to the 3' end of the miRNA; ii) 5'-dominant only, have perfect matching in the seed portion of the 5' end of miRNA; iii) 3' compensatory, have extensive base-pairing of the 3' end of the miRNA to compensate imperfect/mismatch of the miRNA seed portion (Sethupathy, Megraw et al. 2006). From this list of possible mRNA targets, two mRNA with the highest differential expression by qPCR in malignant cell lines were selected for further investigation. We also showed that through the exogenous expression of mature miR-145, we could silence PTGFR mRNA expression as determined by qPCR. In conclusion, miR-145 has the ability to bind the 3' UTR of PTGFR, and silence its expression; which was confirmed by qPCR and the direct-binding assay using a luciferase plasmid. These findings suggest that miR-145 impacts prostate cancer cell growth by targeting genes such as PTGFR.

Sethupathy et al investigated the sensitivity of several target prediction programs and found that the most sensitive programs of the current programs available to the public were miRanda, PicTar, and TargetScanS (Sethupathy, Megraw et al. 2006). In their investigation, the sensitivity was measured as the amount of experimentally supported miRNA targets that are predicted by the program, compared to the total of correctly predicted targets and experimentally supported miRNA targets that were not predicted by the program (Septhupathy, Megraw et al. 2006). If the same test was

carried out only on conserved miRNA targets, the sensitivity further increases for all 3 programs.

Enright first established the miRanda algorithm to detect miRNA targets in *drosophila* and later expanded to include mammalian targets (Enright, John et al. 2003; John, Enright et al. 2004). The miRanda algorithm compares mRNA 3' UTRs to miRNA expressions in three different phases, Phase 1 looks at target selection miRNA:target complementarity matching. In Phase 2, the thermodynamics of the complement sequences are then analyzed. Phase 3 examines the cross-species target site conservation (Enright, John et al. 2003). John et al updated this algorithm to include vertebrate analysis by scanning 3' UTRs from human, mouse, and rat genomes against mammalian miRNA sequences for potential target sites (John, Enright et al. 2004).

TargetScan first searches the orthologus 3' UTRs of humans for segments that have perfect complementarity to the 7 nt seed (bases 2-8 from the 5' end of the miRNA). TargetScan then extends this search to include additional base pairs each direction only allowing G:U pairs until a mismatch occurs. The algorithm then optimizes base pairing of the remaining sequences (3' portion) of the miRNA using the RNAfold program (Schuster, Fontana et al. 1994), this extends the seed match to a longer "target site" (Lewis, Shih et al. 2003). Using RNAeval (Schuster, Fontana et al. 1994), TargetScan assigns folding free energy to each miRNA:target site interaction, and then scores each 3' UTR and applies a rank. This process is then repeated in mouse, and rat 3' UTR, and allows TargetScan to then predict suitable miRNA targets (Lewis, Shih et al. 2003). TargetScan was then improved to TargetScanS by changing

the seed nucleotide match to 6 nt (bases 2-7 from the 5' end of the miRNA) and expanded it's cross-species validation to include chicken and dog genomes without considering any thermodynamic pairing or stability outside the seed position (Lewis, Burge et al. 2005).

Currently, there is no consensus as to which program predicts miRNA targets most accurately. As each program has their advantages and weakness, a combination of two or more programs increases the stringency of selected targets thus increasing the accuracy of the predicted targets. We elected to use two of the most sensitive programs, as determined by Sethupathy's investigation, to more accurately predict miR-145 targets (Sethupathy, Megraw et al. 2006).

With the rapid discovery of miRNA and their targets the demand for databases has also increased proportionally. The earliest compiled database, miRBase, focuses on miRNA data including published miRNA sequences with genomic locations, annotation, and predicted miRNA targets. miRBase also provides a registry to allow researchers to submit their data prior to publication. miRBase has also been updated to include a database of predicted miRNA target genes (Griffiths-Jones, Saini et al. 2004). There are several other examples of currently available databases listed in Table 4.1. These databases function to allow researchers to efficiently gather information on a specific miRNA and it's target. With an individual miRNA controling/regulating hundreds of targets, it remains a challenge to identify the accurate miRNA targets for cancer research. At the moment, the majority of published targets for miRNAs are through in silico searches and algorithms, it is critical that more in vitro assay are developed to confirm these putative targets.

The use of a plasmid expressing luciferase is a common assay used to measure translational inhibition. Clancy et al. outlines a general translational inhibition assay with the use of luciferase plasmid (Clancy, Nousch et al. 2007). Esau and colleagues inserted two miR-143 binding sites into a luciferase expressing plasmid, and found that through the silencing of miR-143 using antisense oligonucleotides, they could rescue transfected cells to express luciferase (Esau, Kang et al. 2004). In another study, miR-221 and -222 was found to have the ability to interact with a cloned fragment of the *kit* mRNA 3' UTR region using a luciferase plasmid transfected into a leukemia cell line (Felli, Fontana et al. 2005). These studies show the feasibility of using a luciferase plasmid assay to examine the interaction of miR-145 and its predicted targets.

Studies have shown that RASSF2 is a potential tumor suppressor gene. In our studies, we discovered that RASSF2 was upregulated in prostate cancer cell lines, which contradicts Vos *et al.*'s finding that RASSF2 regulated K-Ras expression and has the ability to inhibit the growth of lung tumor cells (Vos, Ellis et al. 2003). Interestingly, miR-145 had the ability to decrease RASSF2 mRNA when we examined mRNA expression after miR-145 treatment by qPCR but found that miR-145 did not have the same magnitude of effect on the 3' UTR binding, as seen by the luciferase assay. More studies on RASSF2 and its interaction with miR-145 needs to examined to fully understand miR-145's regulatory effects, and whether a secondary pathway enhances its silencing effect.

The prostagladin F receptor (PTGFR) is a receptor for the protein prostagladin F2α (PGF2α), encoded by the gene *PTGFR.* In Sales and colleagues study, they found,

by real-time PCR and western blotting, that the PGFR expression was found in endometrial adenocarcinoma of all grades and differentiation (Sales, Milne et al. 2004). They found that through PGF2α stimulation the epidermal growth factor receptor (EGFR) could be trans-activated and trigger the MAPK pathway. Interestingly inactivation of phospholipase C (PLC), EGFR kinase, and MAPK kinase using specific inhibitors abolished PGF2α trans-activation of EGFR and MAPK (Sales, Milne et al. 2004). Overexpression of PGF2α also induced the proliferation of human endometrial adenocarcinoma cell line Ishikawa, and introduction of the specific inhibitors against the previously mentioned genes abolished any PGF2α induced cell proliferation (Sales, Milne et al. 2004). It is known that the 1p31 chromosomal region shows loss of heterozygosity (LOH) in 50% of human breast cancers, and *PTGFR* was also mapped to the 1p31 chromosomal region adjacent to the region undergoing LOH, thus showing possible involvement of PTGFR and the progression of human cancers (Sossey-Alaoui, Kitamura et al. 2001). Literature has shown that EGFR inhibition increases radiosensitivity, and contributes to late stage prostate cancer signaling (Liu, Wang et al. 2008; Dehaan, Wolters et al. 2009). Our study suggests that PTGFR may play an important role in prostate cancer advancement through its ability to activate the EGFR and MAPK pathway. No direct connection of PTGFR and prostate cancer has been established, our research is the first to suggest this.

CHAPTER FIVE

Conclusions and Future Studies

As mentioned in Chapter 1, the emphasize of this dissertation was to identify dysregulated miRNAs, especially those that are downregulated, in prostate cancer and examine whether specific miRNAs have an impact on prostate cancer growth and death.

Currently, the data on regarding the miRNA expression profile in prostate cancer is limited. We are one of the first groups to investigate miRNA expression in formalin fixed paraffin embedded (FFPE) prostate cancer. Our study utilized a bead based liquid phase hybridization assay, similar of that described by Lu and coworkers, who first utilized this high throughput method to to successfully classify human cancers and defined the human lung cancer phenotype (Lu, Getz et al 2005). The expression profile of 114 miRNAs from FFPE preserved patient prostate malignant tissue was investigated in our studies and we found that using paired analysis of tumor and normal tissue, 5 miRNAs were significantly downregulated (miR-23b, -100, -145, -221, and -222). These findings were supported by qPCR using primer/probe sets that exclude precursor miRNA amplification.

The ability to use formalin-fixed paraffin embedded tissues is advantageous in that there are no shortage of patient specimens to analyze as many physicians have FFPE tissue archives. In a previous publication, our lab has shown that although mRNA quality and quantity have decreased in FFPE archived tissue, the miRNA

expression has been preserved enough to still reflect their expression profile (Jay, Nemunaitis et al. 2007).

Our preliminary findings indicate that clinically distinct subsets of prostate cancers may be distinguished according to their aggregate miRNA expression profile. The clustering of 75% of early relapse patients according to the expression pattern of 16 miRNAs represents an attractive venue for identifying patients with localized disease and a high likelihood of relapse.

Through the transisent expression of downregulated miRNAs (miR-23b, -145, and -222), we found that these miRNAs had a negative impact on growth in the prostate cancer cell line LNCaP. Interestingly, a combination treatment with miR-23b, -145 and -222 did not significantly increase growth inhibition as compared to single doses of each miRNA. This suggests that these miRNAs might be targeting genes that have overlapping pathways.

Currently, no other studies apart from ours have investigated miR-145 and its possible targets in prostate cancer. Others studies found that miR-145 also had decreased expression in several other solid cancers supports findings that miR-145 might play a role in prostate cancer development (Michael, O'Connor et al. 2003; Bandres, Cubedo et al. 2006; Akao, Nakagawa et al. 2007). In a similar study, Akao and colleagues also found that miR-145 negatively impacts colorectal cancer cell line growth suggesting it's role in tumorgenesis (Akao, Nakagawa et al. 2007). In their studies they found that introduction of precursor miR-145 inhibited cell growth in a dose dependent manner (Akao, Nakagawa et al. 2007).

With the use of *in silico* algorithms we were able to investigate possible miR-145 targets. The miRNA target prediction algorithm TargetScan found 396 targets for miR-145. To select which genes to investigate, we compared the 396 targets against mRNA microarray data analysis of upregulated mRNAs in cancer cell lines and found that several miRNAs were listed in both. We then used current literature to examine which genes might play a relevant role in tumorgenesis. We found that miR-145 directly binds to the 3' UTR of the gene *PTGFR* using a luciferase expression assay. Literature search reveals that *PTGFR* does play a role in tumorgenesis through the activation of EGFR which then in turn triggers the MAPK pathway (Sales, Milne et al. 2004).

In conclusion, our study is one of the first to investigate miRNA expression in FFPE preserved prostate cancer specimens. Through literature review, no other groups have investigated miR-145 and its effect on prostate cancer cell growth. We are the first to report that miR-145 binds directly and silences *PTGFR*, which possible functions as a oncogene through the activation of the EGFR and MAPK pathway.

Future Studies

My studies serve as a foundation for defining possible miRNA targets of miR-145. Since the exact mechanisms of how miRNAs function are still under investigation further studies are needed to establish the exact mechanisms that miR-145 targets and silences its target. In my dissertation, I have not examined the exact mechanism of miR-145 silencing *PTGFR*, whether it is a cleavage dependent or independent mechanism. By defining the exact mechanism of how miR-145

functions in prostate cancer, we can better understand its role in tumor progression. In our studies, we only investigate the downregulation of PTGFR at the mRNA level. We are in the process of investigating miR-145 effects on PTGFR protein expression.

Even though our gene reporter assay did not significantly show the direct binding of RASSF2 by miR-145, our qPCR results indicates that RASSF2 expression is decreased by ectopic expression of miR-145. More studies on the binding of miR-145 to the 3' UTR region of RASSF2 needs to investigated to understand whether RASSF2 is a true target of miR-145.

Our studies serve as a foundation for the investigation of miRNAs and their effects on mRNA targets in prostate cancer involving the use of a high-throughput liquid phase analysis of miRNA expression profile and their effect on mRNA expressions. We are the first to report that PTGFR is a target of miR-145 in the prostate cancer cell line LNCaP.

APPENDICES

APPENDIX A

Trypan Blue Assay Protocol

Reagents needed:

- Trypsin
- 2.0 mL microfuge tubes
- Media for resuspension
- Trypan blue
- Hemacytometer
- Microcentrifuge

Procedure:

1. Remove media from 24 well plate, be sure not to agitate or remove any of the adherent cells at the bottom of the well.
2. Keep the media in a microfuge tube separately.
3. Add 100µL of trypsin to each well.
4. Incubate at 37˚C for 10 mins.
5. Add saved media from step 2, and rinse each well thoroughly and put trypsinized cells in microfuge tube from step 2.
6. Spin down the cells from step 5 for 10 mins at 2400 rpm on a table top micro-centrifuge.

7. Remove as much media as possible without disturbing the cell pellet, which includes both live and dead cells.
8. Re-suspend cells using 100µL of media.
9. Add 10µL of cells to 10µL of trypan blue.
10. Count 4 corners, and center of hemacytometer for death and live cells.
11. Using following formula to calculate number of viable cells.

    (Live cells / 5 x 100 x 2) = total number of viable cells.

APPENDIX B

miR-145 Transfection of LNCaP cells

By Lipofectamine 2000

Reagents needed:

- Lipofectamine 2000 Transfection reagent (Invitrogen, Cat#11668-027)
- Opti-MEM Reduced Serum Media (Invitrogen, Cat#51985-034)
- Microfuge tubes
- RPMI-1640 culture media (ATCC, Cat#30-2001)

Tube Set #1	1x		4x		
Treatment	miR-145 (2µM)	Opti-MEM I	miR-145	Opti-MEM I	Total miRNA (2µM) needed
100nM	25.0	25.0	100.0	100.0	-
50nM	12.5	12.5	50.0	150.0	-
25nM	6.25	43.8	25.0	175.0	175.0
Mock	-	50.0	-	200.0	-
Scrambled	25.0	25.0	100.0	100.0	100.0
UNT	-	-	-	-	-

Tube Set #2	1x	26.4x
Lipofectamine 2000	1.0	26.4
Opti-MEM I	49.0	1293.6
Total	50.0	1320.0

Procedure:

1. One day before transfection, plate cells in 1mL of RPMI-1640 w/10% FBS complete media for LNCaP into 24-well plate at 2 x 10^5 cells/well.
2. For each treatment prepare the following:

a. **Dilute miR-145** according to table for Tube Set #1. **Mix gently**.

b. Mix **Lipofectamine 2000** gently.Then **dilute Lipofectamine 2000 with Opti-MEM I** using table for Tube Set #2. Mix gently and incubate at room temperature for 5 mins. (**Note:** Do not wait longer than 25 mins to proceed to next step).

c. **After 5 mins of incubation**, **combine solution in step 2a. with step 2b**. and **mix gently. Incubate for 20 mins** at room temperature (solution may appear cloudy).

3. **Remove 500µL of media from each well of cell culture in step 1**.

4. **Add mixed solution from step 2c**. to each well containing cells and medium. **Mix gently by rocking back and forth.**

Notes:

- For each treatment, 2 wells were treated (duplicates) to ensure a higher yield during RNA isolation.
- 6 treatments, 2 days, and duplicates = 24 wells needed for experiment.
- RNA will be isolated at 24hrs and 48hrs post-transfection.

By siPORT NeoFX

Reagents needed:

- siPORT NeoFX (Ambion, Cat#AM4511)
- Opti-MEM Reduced Serum Media (Invitrogen, Cat#51985-034)
- Microfuge tubes

- RPMI-1640 culture media (ATCC, Cat#30-2001)

Tube Set #1	1x		20x		
Treatment	miR-145 (2µM)	Opti-MEM I	miR-145	Opti-MEM I	Total miRNA (2µM) needed
50nM	50.0	150.0	200.0	600.0	200.0
Mock	-	200.0	-	800.0	-
Scrambled	50.0	150.0	200.0	600.0	200.0
UNT	-	-	-	-	-

Tube Set #2	1x	60x
siPORT NeoFX	0.5	30.0
Opti-MEM I	9.5	570.0
Total	10.0	600.0

Procedure:

1. Mix siPORT mixture (Tube Set#2) and incubate for 10mins.
2. Dilute miRNA using Opti-MEM to 2µM.
3. Mix miRNA mixture (Tube Set#1)
4. Add equal volumes of siPORT mix (from step 2) to miRNA mix (from step 3).
5. Incubate for 10 mins.
6. Dispense 50µL of step 4 into wells.
7. Add 450µL of cell suspension.

APPENDIX C

PCR conditions for psi-PTGFR and psi-RASSF2 cloning

Reagents needed:

- GoTaq DNA Polymerase (Promega, Cat#M8291)
- Forward and Reverse were ordered from IDT (Integrated DNA Technologies)
- 10mM dNTP (BioRad, Cat#170-8874)
- PCR Thermal cycler
- PCR tubes

Reagent	μL/Rxn	
	1x	2.2x
GoTaq Flexi Buffer	10	22.0
25mM $MgCl_2$	2	4.4
10mM dNTP (Bio-Rad)	1	2.2
Forward Primer (10μM)	2	4.4
Reverse Primer (10μM)	2	4.4
GoTaq DNA Polymerase (5U/μL)	1	2.2
Template DNA	10	22.0
Water	22	48.4
Total Volume	50	110.0

Cycle Step	Temp.	Time	Number of Cycles
Initial Denaturation	94˚C	1 mins	1
Denaturation	94˚C	1 mins	
Annealing	48˚C	30 secs	25-35
Extension	72˚C	30 secs	
Final Extension	72˚C	9 min	
Hold	4˚C	∞	

PCR of **PTGFR** and **RASSF2** 3'UTR from Hela and LNCaP PCR product from previous experiment (Product has 3'UTR but no insertion sites).

- Prepare **2 master mix**, one for each gene (PTGFR, and RASSF2)
- 2 rxns and 1 negative control/gene
- PCR annealing temperature to 48˚C using primer set with digestion sites. (Use low melt temp to get good product yield).
- Increased template DNA to 100ng/rxn

Primer	T_m	Base Pairs
PTGFR 3' UTR Forward	56.3˚C	20
PTFGR 3' UTR Reverse	53.8˚C	22
PTGFR 3' UTR Forward XhoI	62.9˚C	26
PTGFR 3' UTR Reverse NotI	67.5˚C	30
RASSF2 3' UTR Forward	56.0˚C	20
RASSF2 3' UTR Reverse	56.5˚C	20
RASSF2 3' UTR Forward XhoI	60.6˚C	27
RASSF2 3' UTR Reverse NotI	69.3˚C	28

Reagents List for Cloning:

- XhoI restriction endonuclease (New England Biolabs, Cat#R0146L)
- NotI restriction endonuclease (New England Biolabs, Cat#R0189L)
- Quick Ligation (New England Biolabs, Cat#M2200L)
- E-Gel 0.8% Starter Pak (Invitrogen, Cat#G6000-08)
- E-Gel 1.2% General Purpose Agarose 18-Pak (Invitrogen, Cat#G5018-01)
- Microfuge tubes
- QIAquick Gel Extraction Kit (Qiagen, Cat#28706)
- OneShot Max Efficiency DH5α-T1R Competent Cells (Invitrogen, Cat#12297-016)

DNA Digestion

1. Mix the following:

2. 1-2µg (5-10µl) with 1µl restriction enzyme
3. 2µl 10x buffer
4. Add water to a final volume = 20µl.
5. Incubate at 37˚C

DNA Ligation

1. Combine 50 ng of vector with a 3-fold molar excess of insert. Adjust volume to 10 µl with dH2O.
2. Add 10 µl of 2X Quick Ligation Buffer and mix.
3. Add 1µl of Quick T4 DNA Ligase and mix thoroughly.
4. Centrifuge briefly and incubate at room temperature (25°C) for 5 minutes.
5. Chill on ice, then transform or store at -20°C.
6. Do not heat inactivate. Heat inactivation dramatically reduces transformation efficiency.

APPENDIX D

Sequences

PTGFR 3' UTR Target Site (NM_001039585 Total Length 5431)

3' UTR Length: 5431

Position 1504-1511 of PTGFR 3' UTR
5' ...AAAUACCUGUAGCCUAACUGGAA...
hsa-miR-145
3' UUCCCUAAGGACCCUU--UUGACCUG

AACTGGAA = miR-145 8mer target

Forward Primer: 5' GTGGAGTGCATGTCATCAGC 3' (GC = 55% Tm = 60.2˚C)
with XhoI 5' CTCGAGGTGGAGTGCATGTCATCAGC
Reverse Primer: 5' GCTGCATTAAGATGTTCTCTGG 3' (GC = 45.4% Tm= 58.9˚C)
with NotI 5' GCGGCCGCGCTGCATTAAGATGTTCTCTGG

Product Size: 460bp

GTGGAGTGCATGTCATCAGCTTACATATTTGGGAGCTTAGTTCCATTAAAA
ATTCCTTAAAGGTTGCTGCTATTTCTGAGTCACCAGTTGCAGAGAAATCAG
CAAGCACCTAGCTTAATAGGACAGTAAATCTGTGTGGGGCTAGAACAAAA
TTAAGACATGTTTGGCAATATTTCAGTTAGTTAAATACCTGTAGCCTAACTG
GAAAATTCAGGCTTCATCATGTAGTTTGAAGATACTATTGTCAGATTCAGG
TTTTGAAATTTGTCAAATAAACAGGATAACTGTACATTTTTCACTTGTTTTT
GCCAATGGGAGGTAGACACAATAAAATAATGCCATGGGAGTCACACTGAA
AGCAATTTTGAGCTTATCTGTCTTATTTATGCTTTGAGTGAATCATCTGTTG
AGGTCTAATGCCTTTACTTGGCCTATTTGCCAGAGAACATCTTAATGCAGC

RASSF2 3' UTR Target Site (NM_014737 Total Length 5426)

3' UTR Length: 5426

Position 4695-4700 of PTGFR 3' UTR
5' ...CCCACGUAUUUUUAC----ACUGGAAA...

hsa-miR-145
3' UUCCCUAAGGACCCUUUUGACCUG

UGACCU = miR-145 7mer-1A target

Forward Primer: 5' CTCAGCTCACTGCAACATCC 3' (GC = 55.0% Tm = 59.5˚C)
with XhoI 5' CTCGAGTGATCTGAGACATGCTGATGC

Reverse Primer: 5' ACAGCTTGTGCATCTTGTGC 3'(GC = 50% Tm = 60.0˚C)
with NotI 5' GCGGCCGCACAGCTTGTGCATCTTGTGC

Product Size: 567bp

CTCAGCTCACTGCAACATCCGCCTCTGGGGTTCAAGTGATTCTCCTGTCTCA
GCCTCCCAAGTAGCTGGAATTACAGGGACCCGCCACCACGCCCGGCTAATT
TTTTTGTGTGGTTTTAGTAGAGGTGGGGTTTCACCATCTTGGCCAGGCTGGT
CTTGAACTCCTGACCTCGTGATCCACCCGCCTAGGCCTCCCAAAGTGTTGG
GATTACAGGCGTGAGCCACTGTGCCCAGCCAAAAGAGAAATTTCTACATGA
ACAAGGCAATTTCAGTGTCTTACAGCGGCCAAACCATGACGTGAAGAATG
AGATAGGAGACAGGAGATCACCATAAGCGTCCCTGATATAGCAGCACACA
TTTTCACGTTTCCACTTAAATCGTTTTGCACAAAGTCTTGCTTCGCTCAGAT
GAGATGAGATATGATTTCCTAGAGATGTAAAAATAAGAATGAATGTGGCG
CCCCCTTCTTCCAGATGTAATAGAAAGCTCTGCCCTATCACAAGGGGGGTG
TTGAAGCGCCCCTTGTGTTTTAACTGTATTTAACTGAGCACAAGATGCACA
AGCTGT

PTGFR (Sequenced data)

CTCGAGGTGGAGTGCATGTCATCAGCTTACATATTTGGGAGCTTAGTTCCA
TTAAAAATTCCTTAAAGGTTGCTGCTATTTCTGAGTCACCAGTTGCAGAGA
AATCAGCAAGCACCTAGCTTAATAGGACAGTAAATCTGTGTGGGGCTAGA
ACAAAATTAAGACATGTTTGGCAATATTTCAGTTAGTTAAATACCTGTAGC
CTAACTGGAAAATTCAGGCTTCATCATGTAGTTTGAAGATACTATTGTCAG
ATTCAGGTTTTGAAATTTGTCAAATAAACAGGATAACTGTACATTTTTCACT
TGTTTTTGCCAATGGGAGGTAGACACAATAAAATAATGCCATGGGAGTCAC
ACTGAAAGCAATTTTGAGCTTATCTGTCTTATTTATGCTTTGAGTGAATCAT
CTGTTGAGGTCTAATGCCTTTACTTGGCCTATTTGCCAGAGAACATCTTAAT
GCAGC

RASSF2 (Sequenced data)

CTCAGCTCACTGCAACATCCGCCTCTGGGGTTCAAGTGATTCTCCTGTCTCA
GCCTCCCAAGTAGCTGGAATTACAGGGACCCGCCACCACGCCCGGCTAATT
TTTTTGTGTGGTTTTAGTAGAGGTGGGGTTTCACCATCTTGGCCAGGCTGGT
CTTGAACTCCTGACCTCGTGATCCACCCGCCTAGGCCTCCCAAAGTGTTGG
GATTACAGGCGTGAGCCACTGTGCCCAGCCAAAAGAGAAATTTCTACATGA
ACAAGGCAATTTCAGTGTCTTACAGCGGCCAAACCATGACGTGAAGAATG
AGATAGGAGACAGGAGATCACCATAAGCGTCCCTGATATAGCAGCACACA
TTTTCACGTTTCCACTTAAATCGTTTTGCACAAAGTCTTGCTTCGCTCAGAT
GAGATGAGATATGATTTCCTAGAGATGTAAAAATAAGAATGAATGTGGCG
CCCCCTTCTTCCAGATGTAATAGAAAGCTCTGCCCTATCACAAGGGGGGTG
TTGAAGCGCCCCTTGTGTTTTAACTGTATTTAACTGAGCACAAGATGCACA
AGCTGT

APPENDIX E

UT Southwestern Affymetrix Gene Array Protocol
Eukaryotic Target Hybridization

Reagents and Materials Required

The following reagents and materials are recommendations:

- DEPC- Treated Water. Ambion Cat.#9922
- Bovine Serum Albumin (BSA) solution (50 mg/mL), Invitrogen Life Technologies, P/N 15561-020
- Herring Sperm DNA, Promega Corporation, P/N D1811
- GeneChip Eukaryotic Hybridization Control Kit, Affymetrix, P/N 900454 (30 reactions) or P/N 900457 (150 reactions), contains Control cRNA and Control Oligo B2
- Control Oligo B2, 3 nM, Affymetrix, P/N 900301 (can be ordered separately)
- 5M NaCl, RNase-free, DNase-free, Ambion, P/N 9760G
- MES hydrate SigmaUltra, Sigma-Aldrich, P/N M5287
- MES Sodium Salt, Sigma-Aldrich, P/N M5057
- EDTA Disodium Salt, 0.5M solution (100 mL), Sigma-Aldrich, P/N E7889
- DMSO, Sigma-Aldrich, P/N D5879
- Surfact-Amps 20 (Tween-20), 10%, Pierce Chemical, P/N 28320

Miscellaneous Supplies

- Hybridization Oven 640, Affymetrix, P/N 800138 (110V) or 800139 (220V)
- Sterile, RNase-free, microcentrifuge vials, 1.5 mL, USA Scientific, P/N 1415-2600 (or equivalent)
- Micropipettors, (P-2, P-20, P-200, P-1000), Rainin Pipetman (or equivalent)
- Sterile-barrier pipette tips and non-barrier pipette tips
- Heatblock (Fisher-scientific)
- Thermometer

Reagent Preparation

12X MES Stock Buffer

(1.22M MES, 0.89M [Na+])

For 1,000 mL: 64.61g of MES hydrate, 193.3g of MES Sodium Salt, 800 mL of Molecular Biology Grade water.

Mix and adjust volume to 1,000 mL.

The pH should be between 6.5 and 6.7. Filter through a 0.2 m filter.

2X Hybridization Buffer

(Final 1X concentration is 100 mM MES, 1M [Na+], 20 mM EDTA, 0.01% Tween-20)

For 50 mL: 8.3 mL of 12X MES Stock Buffer 17.7 mL of 5M NaCl 4.0 mL of 0.5M EDTA, 0.1 mL of 10% Tween-20, 19.9 mL of water, Store at 4 C, and shield from light.

Eukaryotic Target fragmentation and Hybridization

1. Calculate the necessary amount of cRNA 20ug (cRNA concentration at least 0.625ug/ul) Place in 0.5ml tubes. Adjust volume to 32ul with nuclease free water.
2. Add 8ul of 5x Fragmentation buffer to each sample. Vortex, spin briefly.
3. Incubate at 94C for 35 minutes in the heat block.
4. While cRNA is fragmenting, take out Gene Chips and place them at room temperature. *It is important to allow the chips to equilibrate to room temperature completely. Specifically, if the rubber septa are not equilibrated to room temperature, they may be prone to cracking, which can lead to leaks. Usually takes about 20 minutes.*
5. Incubate the probe array filled with 1X Hybridization Buffer at 45C for 10 minutes with rotation.
    - 49 Format (Standard) 200ul
    - 64 Format 200 ul
    - 100 Format (Midi) 130 ul
    - 169 Format (Mini) 80 ul
    - 400 Format (Micro) 80 ul
    - Place Chips at 45C in Hybridization oven, rotating at 60 rpm. for 10 minutes.
6. When 35 min is up remove samples from heat block and spin down .
7. Add the following reagents
    a. 5ul of Oligo B2

b. 15 ul of 20x Eukaryotic Controls (It is imperative that frozen stocks of 20X
c. GeneChip Eukaryotic Hybridization Controls are heated to 65C for 5 minutes to completely resuspend the cRNA before aliquotting)
d. 3ul of herring Sperm DNA
e. 3ul of BSA
f. 84 ul of Nuclease free water
g. 150 ul of 2x Hybridization Buffer
h. Vortex,Spin briefly.

8. Heat the hybridization cocktail to 99C for 5 minutes in a heat block.
9. Transfer the hybridization cocktail that has been heated at 99C, to a 45C oven for 5 minutes.
10. Spin hybridization cocktail(s) at maximum speed in a microcentrifuge for 5 minutes to remove any insoluble material from the hybridization mixture.
11. Remove the buffer solution from the probe array cartridge and fill with appropriate volume (Table 2.2.2) of the clarified hybridization cocktail, avoiding any insoluble matter at the bottom of the tube.
12. Place probe array into the Hybridization Oven, set to 45C. Avoid stress to the motor; load probe arrays in a balanced configuration around the axis. Rotate at 60 rpm.
13. Hybridize for 16-18 hours.

APPENDIX F

Transfection Efficiency

gWiz GFP Plasmid
used 1ug/well

3/13/07
24 wells

$4.5x10^4$ cells
LNCaP
1uL siPORT/well

gWiz Transfected	Fluoresence Cells	Total Viable Cells	Dead Cells		% Fluorescent
1	130	348	53		37.36
2	199	431	45		46.17
3	113	316	49		35.76
4	138	294	46		46.94
Total cells	580	1389	193	Mean	41.56
Mean	145	347.3	48.3	SD	5.82
SD	37.5	60.1	3.6		
	% Fluorescent	41.76			

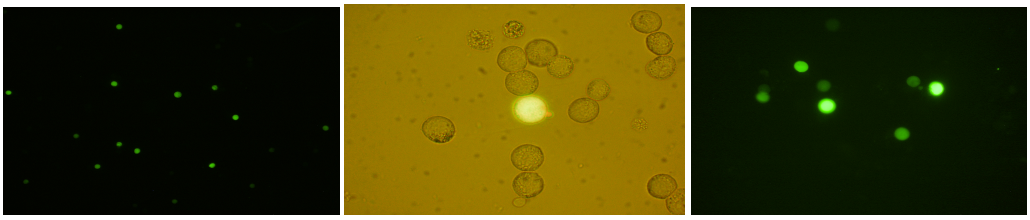

Left: LNCaP cells treated with gWiz GFP plasmid and viewed under fluorescent microscope, 40x

Middle: LNCaP cells viewed under microscope with fluorescence to count for total cells and fluorescent cells, 200x

Right: LNCaP cells treated with qWiz GFP plasmid viewed under 200x

Appendix G

qPCR Validation of miRNA Expression in Relapse vs Non-relapse Patients

Data Summary: 6 microRNAs' Expression Data Statistical Analysis by qRT-PCR and Comparison between qRT-PCR Data and mirMASA Data
22 Patients(I) iQ5 Gene Study Data **Normalized by RNU44** T/N ratio presented for each patient and microRNA
Data Sorce: Copied form "071808_iQ5 Gene Study Analyzed"
Date: 07/23/008-/07/24/08 SL

T/N Ratio

		Normalized by RNU44						mirMASA normalized by 5S RNA					
		Supposed to be up-regulated				Supposed to be down-regulated		Supposed to be up-regulated				Supposed to be down-regulated	
		miR-16	miR-135b	miR-194	miR-218	miR-140	miR-342	miR-16	miR-135b	miR-194	miR-218	miR-140	miR-342
Non-relapse	17	0.085	0.191	0.105	0.153	0.173	0.102	0.654	0.260	1.234	0.306	0.074	
	33	0.313	0.415	0.277	0.436	0.430	0.336	0.990	0.895	0.387	1.341	1.604	0.225
	47	0.392	0.746	0.598	0.666	0.498	0.379	1.292	1.119	0.802	1.056	0.517	1.230
	51	0.666	0.452	0.254	0.488	0.604	0.436	1.523	0.964	0.715	1.196	0.762	0.552
	84	1.780	1.315	1.307	2.043	4.743	2.346	1.176	0.950	0.956	0.715	0.917	1.546
	89	2.839	1.189	1.848	1.942	3.496	1.764	1.355	1.160	1.012	1.382	1.557	0.922
	14	0.328	0.576	0.373	0.389	0.392	0.285	0.015		0.897	1.035		0.272
	19	0.411	2.361	0.293	0.429	0.400	0.288	1.440		0.674	0.600	3.556	1.026
	21	0.490	0.978	0.521	0.720	0.171	0.526	0.915	1.260	0.888	0.199	0.770	
	27	0.425	1.323	0.544	0.377	0.501	0.522	0.362	0.000	0.474	0.850	0.939	1.110
	58	0.297	1.812	0.268	0.377	0.305	0.285	0.705	1.232	0.649	0.601	4.853	1.163
Relapse	12	0.479	0.443	0.458	0.778	1.097	0.731	0.799	1.555	2.697	1.705	2.520	1.207
	23	0.251	0.326	0.287	0.308	0.171	0.401	0.843	1.096	0.860	0.774	0.931	1.346
	69	0.468	1.134	0.123	1.364	0.481	0.167	0.763	1.879	1.422	1.198	1.231	0.492
	72	1.071	1.756	0.451	0.877	0.884	0.703	0.800	30.565	1.091	2.683	1.357	1.647
	78	0.280	0.302	0.692	0.491	0.642	0.815	1.289	0.965	0.652	1.090	1.073	1.615

	86	2.698	8.007	2.070	2.584	2.780	3.496	0.597	1.609	1.203	1.079	1.062	0.926
	11	0.350	0.620	0.258	0.494	0.473	0.459	2.746	0.435	1.572	1.011	0.612	0.742
	75	0.546	0.351	0.567	0.402	0.448	0.743	0.783	0.463	1.028	0.669	0.904	0.818
	76	1.505	1.551	2.336	0.937	0.468	1.235	1.320	1.353	1.558	0.865	1.213	0.860
	85	0.985	1.504	1.094	0.870	1.627	0.553	0.620	4.787	0.633	0.927	1.321	0.861
	92	0.375	1.623	0.812	0.364	0.487	0.248	0.873	1.223	0.935	1.609	0.686	0.921
Column Statistics													
R Average		0.819	1.602	0.832	0.861	0.869	0.868	1.039	4.175	1.241	1.237	1.173	1.039
R SD		0.737	2.202	0.733	0.653	0.749	0.920	0.612	8.830	0.582	0.576	0.508	0.367
NR Average		0.729	1.033	0.581	0.729	1.065	0.661	0.948	0.871	0.790	0.844	1.555	0.894
NR SD		0.828	0.654	0.528	0.643	1.541	0.712	0.476	0.443	0.244	0.398	1.498	0.451
R/NR Ratio		1.123	1.551	1.432	1.181	0.816	1.314	1.096	4.794	1.571	1.466	0.755	1.163
R vs NR, t-test		0.792	0.421	0.368	0.638	0.709	0.561	0.700	0.279	0.028	0.077	0.435	0.437
R vs NR, Mann Whitney test		0.599	0.948	0.325	0.325	0.341	0.212	0.708	0.027	0.046	0.100	0.926	0.921
qRT-PCR vs mirMASA													
matched pairs		15	14	14	12	13	9						
paired t-test		0.273	0.365	0.068	0.145	0.334	0.392						

Conclusion:

1. All six miRNAs have the same trend of R/NR ratio between qRT-PCR and mirMASA: five miRNAs were up-regulated in relapse group (miR-16, miR-135b, miR-194, miR-218 and miR-342), and one miRNA was down-regulated (miR-140).
2. Statistical analysis to compare qRT-PCR and mirMASA data on the agreement of the two set of data: paired t-test: all six miRNAs show agreement.

Conclusion:

1. All six miRNAs have the same trend of R/NR ratio between qRT-PCR and mirMASA: five miRNAs were up-regulated in relapse group (miR-16, miR-135b, miR-194, miR-218 and miR-342), and one miRNA was down-regulated (miR-140).
2. Statistical analysis to compare qRT-PCR and mirMASA data on the agreement of the two set of data: paired t-test: all six miRNAs show agreement.
3. Significantly different T/N ratios between relapse group and non-relapse group can only be seen for miR-194, in mirMASA data. Other five miRNAs do not show significant difference in mirMASA data.
4. Data by qRT-PCR do not show that any of the six miRNAs have significantly different T/N ratios between relapse group and non-relapse group. (Mann-Whitney test).

REFERENCES

American Cancer Society 2008. Cancer Facts and Figures 2008. American Cancer Society.

Akao Y, Nakagawa Y, Naoe T. 2006. let-7 microRNA functions as a potential growth suppressor in human colon cancer cells. Biol Pharm Bull 29(5):903-6.

Akao Y, Nakagawa Y, Naoe T. 2007. MicroRNA-143 and -145 in colon cancer. DNA Cell Biol 26(5):311-20.

Ambros V. 2003. MicroRNA pathways in flies and worms: growth, death, fat, stress, and timing. Cell 113(6):673-6.

Bandres E, Cubedo E, Agirre X, Malumbres R, Zarate R, Ramirez N, Abajo A, Navarro A, Moreno I, Monzo M and others. 2006. Identification by Real-time PCR of 13 mature microRNAs differentially expressed in colorectal cancer and non-tumoral tissues. Mol Cancer 5:29.

Barad O, Meiri E, Avniel A, Aharonov R, Barzilai A, Bentwich I, Einav U, Gilad S, Hurban P, Karov Y and others. 2004. MicroRNA expression detected by oligonucleotide microarrays: system establishment and expression profiling in human tissues. Genome Res 14(12):2486-94.

Bohnsack MT, Czaplinski K, Gorlich D. 2004. Exportin 5 is a RanGTP-dependent dsRNA-binding protein that mediates nuclear export of pre-miRNAs. RNA 10(2):185-91.

Bradford TJ, Tomlins SA, Wang X, Chinnaiyan AM. 2006. Molecular markers of prostate cancer. Urol Oncol 24(6):538-51.

Brueckner B, Stresemann C, Kuner R, Mund C, Musch T, Meister M, Sultmann H, Lyko F. 2007. The human let-7a-3 locus contains an epigenetically regulated microRNA gene with oncogenic function. Cancer Res 67(4):1419-23.

Calin GA, Croce CM. 2006. MicroRNAs and chromosomal abnormalities in cancer cells. Oncogene 25(46):6202-10.

Calin GA, Dumitru CD, Shimizu M, Bichi R, Zupo S, Noch E, Aldler H, Rattan S, Keating M, Rai K and others. 2002. Frequent deletions and down-regulation of micro- RNA genes miR15 and miR16 at 13q14 in chronic lymphocytic leukemia. Proc Natl Acad Sci U S A 99(24):15524-9.

Calin GA, Ferracin M, Cimmino A, Di Leva G, Shimizu M, Wojcik SE, Iorio MV, Visone R, Sever NI, Fabbri M and others. 2005. A MicroRNA signature associated with prognosis and progression in chronic lymphocytic leukemia. N Engl J Med 353(17):1793-801.

Calin GA, Sevignani C, Dumitru CD, Hyslop T, Noch E, Yendamuri S, Shimizu M, Rattan S, Bullrich F, Negrini M and others. 2004. Human microRNA genes are frequently located at fragile sites and genomic regions involved in cancers. Proc Natl Acad Sci U S A 101(9):2999-3004.

Chan J, Krichevsky A, Kosik K. 2005. MicroRNA-21 is an antiapoptotic factor in human glioblastoma cells. Cancer Res 65(14):6029-33.

Cho WC. 2007. OncomiRs: the discovery and progress of microRNAs in cancers. Mol Cancer 6:60.

Ciafre SA, Galardi S, Mangiola A, Ferracin M, Liu CG, Sabatino G, Negrini M, Maira G, Croce CM, Farace MG. 2005. Extensive modulation of a set of microRNAs in primary glioblastoma. Biochem Biophys Res Commun 334(4):1351-8.

Clancy JL, Nousch M, Humphreys DT, Westman BJ, Beilharz TH, Preiss T. 2007. Methods to analyze microRNA-mediated control of mRNA translation. Methods Enzymol 431:83-111.

Coller HA, Forman JJ, Legesse-Miller A. 2007. "Myc'ed messages": myc induces transcription of E2F1 while inhibiting its translation via a microRNA polycistron. PLoS Genet 3(8):e146.

Cooper WN, Dickinson RE, Dallol A, Grigorieva EV, Pavlova TV, Hesson LB, Bieche I, Broggini M, Maher ER, Zabarovsky ER and others. 2008. Epigenetic regulation of the ras effector/tumour suppressor RASSF2 in breast and lung cancer. Oncogene 27(12):1805-11.

Dehaan AM, Wolters NM, Keller ET, Ignatoski KM. 2009. EGFR ligand switch in late stage prostate cancer contributes to changes in cell signaling and bone remodeling. Prostate.

Dong J, Boyd J, Frierson H. 2001. Loss of heterozygosity at 13q14 and 13q21 in high grade, high stage prostate cancer. Prostate 49(3):166-71.

Endoh M, Tamura G, Honda T, Homma N, Terashima M, Nishizuka S, Motoyama T. 2005. RASSF2, a potential tumour suppressor, is silenced by CpG island hypermethylation in gastric cancer. Br J Cancer 93(12):1395-9.

Enright AJ, John B, Gaul U, Tuschl T, Sander C, Marks DS. 2003. MicroRNA targets in Drosophila. Genome Biol 5(1):R1.

Esau C, Kang X, Peralta E, Hanson E, Marcusson EG, Ravichandran LV, Sun Y, Koo S, Perera RJ, Jain R and others. 2004. MicroRNA-143 regulates adipocyte differentiation. J Biol Chem 279(50):52361-5.

Esquela-Kerscher A, Slack FJ. 2006. Oncomirs - microRNAs with a role in cancer. Nat Rev Cancer 6(4):259-69.

Felli N, Fontana L, Pelosi E, Botta R, Bonci D, Facchiano F, Liuzzi F, Lulli V, Morsilli O, Santoro S and others. 2005. MicroRNAs 221 and 222 inhibit normal erythropoiesis and erythroleukemic cell growth via kit receptor down-modulation. Proc Natl Acad Sci U S A 102(50):18081-6.

Gaur A, Jewell D, Liang Y, Ridzon D, Moore J, Chen C, Ambros V, Israel M. 2007. Characterization of microRNA expression levels and their biological correlates in human cancer cell lines. Cancer Res 67(6):2456-68.

Giraldez AJ, Mishima Y, Rihel J, Grocock RJ, Van Dongen S, Inoue K, Enright AJ, Schier AF. 2006. Zebrafish MiR-430 promotes deadenylation and clearance of maternal mRNAs. Science 312(5770):75-9.

Gong H, Liu CM, Liu DP, Liang CC. 2005. The role of small RNAs in human diseases: potential troublemaker and therapeutic tools. Med Res Rev 25(3):361-81.

Griffiths-Jones S, Saini HK, van Dongen S, Enright AJ. 2008. miRBase: tools for microRNA genomics. Nucleic Acids Res 36(Database issue):D154-8.

Grun D, Wang YL, Langenberger D, Gunsalus KC, Rajewsky N. 2005. microRNA target predictions across seven Drosophila species and comparison to mammalian targets. PLoS Comput Biol 1(1):e13.

Harfe BD. 2005. MicroRNAs in vertebrate development. Curr Opin Genet Dev 15(4):410-5.

He H, Jazdzewski K, Li W, Liyanarachchi S, Nagy R, Volinia S, Calin GA, Liu CG, Franssila K, Suster S and others. 2005. The role of microRNA genes in papillary thyroid carcinoma. Proc Natl Acad Sci U S A 102(52):19075-80.

Iorio MV, Ferracin M, Liu CG, Veronese A, Spizzo R, Sabbioni S, Magri E, Pedriali M, Fabbri M, Campiglio M and others. 2005. MicroRNA gene expression deregulation in human breast cancer. Cancer Res 65(16):7065-70.

John B, Enright AJ, Aravin A, Tuschl T, Sander C, Marks DS. 2004. Human MicroRNA targets. PLoS Biol 2(11):e363.

Johnson SM, Grosshans H, Shingara J, Byrom M, Jarvis R, Cheng A, Labourier E, Reinert KL, Brown D, Slack FJ. 2005. RAS is regulated by the let-7 microRNA family. Cell 120(5):635-47.

Kaira K, Sunaga N, Tomizawa Y, Yanagitani N, Ishizuka T, Saito R, Nakajima T, Mori M. 2007. Epigenetic inactivation of the RAS-effector gene RASSF2 in lung cancers. Int J Oncol 31(1):169-73.

Khvorova A, Reynolds A, Jayasena SD. 2003. Functional siRNAs and miRNAs exhibit strand bias. Cell 115(2):209-16.

Kiriakidou M, Nelson PT, Kouranov A, Fitziev P, Bouyioukos C, Mourelatos Z, Hatzigeorgiou A. 2004. A combined computational-experimental approach predicts human microRNA targets. Genes Dev 18(10):1165-78.

Krek A, Grun D, Poy MN, Wolf R, Rosenberg L, Epstein EJ, MacMenamin P, da Piedade I, Gunsalus KC, Stoffel M and others. 2005. Combinatorial microRNA target predictions. Nat Genet 37(5):495-500.

Lall S, Grun D, Krek A, Chen K, Wang YL, Dewey CN, Sood P, Colombo T, Bray N, Macmenamin P and others. 2006. A genome-wide map of conserved microRNA targets in C. elegans. Curr Biol 16(5):460-71.

Lau NC, Lim LP, Weinstein EG, Bartel DP. 2001. An abundant class of tiny RNAs with probable regulatory roles in Caenorhabditis elegans. Science 294(5543):858-62.

Lee RC, Feinbaum RL, Ambros V. 1993. The C. elegans heterochronic gene lin-4 encodes small RNAs with antisense complementarity to lin-14. Cell 75(5):843-54.

Lewis BP, Burge CB, Bartel DP. 2005. Conserved seed pairing, often flanked by adenosines, indicates that thousands of human genes are microRNA targets. Cell 120(1):15-20.

Lewis BP, Shih IH, Jones-Rhoades MW, Bartel DP, Burge CB. 2003. Prediction of mammalian microRNA targets. Cell 115(7):787-98.

Lim LP, Lau NC, Garrett-Engele P, Grimson A, Schelter JM, Castle J, Bartel DP, Linsley PS, Johnson JM. 2005. Microarray analysis shows that some microRNAs downregulate large numbers of target mRNAs. Nature 433(7027):769-73.

Liu F, Wang JJ, You ZY, Zhang YD, Zhao Y. 2008. Radiosensitivity of prostate cancer cells is enhanced by EGFR inhibitor C225(). Urol Oncol.

Lu J, Getz G, Miska EA, Alvarez-Saavedra E, Lamb J, Peck D, Sweet-Cordero A, Ebert BL, Mak RH, Ferrando AA and others. 2005. MicroRNA expression profiles classify human cancers. Nature 435(7043):834-8.

Lujambio A, Esteller M. 2007. CpG island hypermethylation of tumor suppressor microRNAs in human cancer. Cell Cycle 6(12):1455-9.

Mattie MD, Benz CC, Bowers J, Sensinger K, Wong L, Scott GK, Fedele V, Ginzinger D, Getts R, Haqq C. 2006. Optimized high-throughput microRNA expression profiling provides novel biomarker assessment of clinical prostate and breast cancer biopsies. Mol Cancer 5:24.

Michael MZ, SM OC, van Holst Pellekaan NG, Young GP, James RJ. 2003. Reduced accumulation of specific microRNAs in colorectal neoplasia. Mol Cancer Res 1(12):882-91.

Murakami Y, Yasuda T, Saigo K, Urashima T, Toyoda H, Okanoue T, Shimotohno K. 2006. Comprehensive analysis of microRNA expression patterns in hepatocellular carcinoma and non-tumorous tissues. Oncogene 25(17):2537-45.

Nelson PT, Wang WX, Wilfred BR, Tang G. 2008. Technical variables in high-throughput miRNA expression profiling: much work remains to be done. Biochim Biophys Acta 1779(11):758-65.

Ozen M, Creighton CJ, Ozdemir M, Ittmann M. 2008. Widespread deregulation of microRNA expression in human prostate cancer. Oncogene 27(12):1788-93.

Petersen M, Wengel J. 2003. LNA: a versatile tool for therapeutics and genomics. Trends Biotechnol 21(2):74-81.

Pillai RS. 2005. MicroRNA function: multiple mechanisms for a tiny RNA? RNA 11(12):1753-61.

Porkka KP, Pfeiffer MJ, Waltering KK, Vessella RL, Tammela TL, Visakorpi T. 2007. MicroRNA expression profiling in prostate cancer. Cancer Res 67(13):6130-5.

Rana TM. 2007. Illuminating the silence: understanding the structure and function of small RNAs. Nat Rev Mol Cell Biol 8(1):23-36.

Rehmsmeier M, Steffen P, Hochsmann M, Giegerich R. 2004. Fast and effective prediction of microRNA/target duplexes. RNA 10(10):1507-17.

Rusinov V, Baev V, Minkov IN, Tabler M. 2005. MicroInspector: a web tool for detection of miRNA binding sites in an RNA sequence. Nucleic Acids Res 33(Web Server issue):W696-700.

Saetrom P, Snove O, Jr., Rossi JJ. 2007. Epigenetics and microRNAs. Pediatr Res 61(5 Pt 2):17R-23R.

Saetrom P, Snove O, Nedland M, Grunfeld TB, Lin Y, Bass MB, Canon JR. 2006. Conserved microRNA characteristics in mammals. Oligonucleotides 16(2):115-44.

Sales KJ, Milne SA, Williams AR, Anderson RA, Jabbour HN. 2004. Expression, localization, and signaling of prostaglandin F2 alpha receptor in human endometrial adenocarcinoma: regulation of proliferation by activation of the epidermal growth factor receptor and mitogen-activated protein kinase signaling pathways. J Clin Endocrinol Metab 89(2):986-93.

Schuster P, Fontana W, Stadler PF, Hofacker IL. 1994. From sequences to shapes and back: a case study in RNA secondary structures. Proc Biol Sci 255(1344):279-84.

Sethupathy P, Megraw M, Hatzigeorgiou AG. 2006. A guide through present computational approaches for the identification of mammalian microRNA targets. Nat Methods 3(11):881-6.

Shukla S, Naumov I, Hameiri-Grossman M, Cohen I, Ash S, Yaniv I, Avigad S. 2007. Methylation analysis of specific mirroRNAs in Eqing's Sarcoma (abstract). AACR Proceedings 2007 48:2862.

Sossey-Alaoui K, Kitamura E, Cowell JK. 2001. Fine mapping of the PTGFR gene to 1p31 region and mutation analysis in human breast cancer. Int J Mol Med 7(5):543-6.

Tang G. 2005. siRNA and miRNA: an insight into RISCs. Trends Biochem Sci 30(2):106-14.

Tong AW, Fulgham P, Jay C, Chen P, Khalil I, Liu S, Senzer N, Eklund AC, Han J, Nemunaitis J. 2008. MicroRNA profile analysis of human prostate cancers. Cancer Gene Ther.

Tong AW, Nemunaitis J. 2008. Modulation of miRNA activity in human cancer: a new paradigm for cancer gene therapy? Cancer Gene Ther 15(6):341-55.

van Rooij E, Olson EN. 2007. MicroRNAs: powerful new regulators of heart disease and provocative therapeutic targets. J Clin Invest 117(9):2369-76.

Volinia S, Calin GA, Liu CG, Ambs S, Cimmino A, Petrocca F, Visone R, Iorio M, Roldo C, Ferracin M and others. 2006. A microRNA expression signature of human solid tumors defines cancer gene targets. Proc Natl Acad Sci U S A 103(7):2257-61.

Voorhoeve PM, le Sage C, Schrier M, Gillis AJ, Stoop H, Nagel R, Liu YP, van Duijse J, Drost J, Griekspoor A and others. 2006. A genetic screen implicates miRNA-372 and miRNA-373 as oncogenes in testicular germ cell tumors. Cell 124(6):1169-81.

Vos MD, Ellis CA, Elam C, Ulku AS, Taylor BJ, Clark GJ. 2003. RASSF2 is a novel K-Ras-specific effector and potential tumor suppressor. J Biol Chem 278(30):28045-51.

Walczak JR, Carducci MA. 2007. Prostate cancer: a practical approach to current management of recurrent disease. Mayo Clin Proc 82(2):243-9.

Wang H, He X, Band M, Wilson C, Liu L. 2005. A study of inter-lab and inter-platform agreement of DNA microarray data. BMC Genomics 6(1):71.

Weinstein IB. 2002. Cancer. Addiction to oncogenes--the Achilles heal of cancer. Science 297(5578):63-4.

White RJ. 2004. RNA polymerase III transcription and cancer. Oncogene 23(18):3208-16.

Wu L, Fan J, Belasco JG. 2006. MicroRNAs direct rapid deadenylation of mRNA. Proc Natl Acad Sci U S A 103(11):4034-9.

Xi Y, Shalgi R, Fodstad O, Pilpel Y, Ju J. 2006. Differentially regulated micro-RNAs and actively translated messenger RNA transcripts by tumor suppressor p53 in colon cancer. Clin Cancer Res 12(7 Pt 1):2014-24.

Yang L, Tran DK, Wang X. 2001. BADGE, Beads Array for the Detection of Gene Expression, a high-throughput diagnostic bioassay. Genome Res 11(11):1888-98.

Zeng Y, Yi R, Cullen BR. 2003. MicroRNAs and small interfering RNAs can inhibit mRNA expression by similar mechanisms. Proc Natl Acad Sci U S A 100(17):9779-84.

Zhang L, Huang J, Yang N, Greshock J, Megraw MS, Giannakakis A, Liang S, Naylor TL, Barchetti A, Ward MR and others. 2006a. microRNAs exhibit high frequency genomic alterations in human cancer. Proc Natl Acad Sci U S A 103(24):9136-41.

Zhang YA, Nemunaitis J, Samuel SK, Chen P, Shen Y, Tong AW. 2006b. Antitumor activity of an oncolytic adenovirus-delivered oncogene small interfering RNA. Cancer Res 66(19):9736-43.